Omega 133 (2025) 103264

Contents lists available at ScienceDirect

Omega

journal homepage: www.elsevier.com/locate/omega

A comprehensive methodology combining machine learning and unified robust stochastic programming for medical supply chain viability☆

Ömer Faruk Yılmaz [a,b,*], Yongpei Guan [c], Beren Gürsoy Yılmaz [a,d], Fatma Betül Yeni [a], Gökhan Özçelik [a]

[a] Department of Industrial Engineering, Karadeniz Technical University, Trabzon 61080, Turkey
[b] Department of Industrial and Systems Engineering, Center for Applied Optimization, University of Florida, Gainesville, FL, USA
[c] Department of Industrial and Systems Engineering, University of Florida, Gainesville, FL, USA
[d] Department of Industrial and Systems Engineering, Supply Chain and Logistics Engineering Laboratory, University of Florida, Gainesville, FL, USA

ARTICLE INFO

Edited by Prof. Benjamin Lev

Keywords:
Medical supply chain
Kit allocation problem
Unified robust stochastic programming
Machine learning
Contagion impact of disease

ABSTRACT

This paper addresses the medical kit allocation problem by employing a unified robust stochastic programming (URSP) approach to enhance medical supply chain (MSC) viability during pandemics. A two-stage methodology is developed to account for the inherent uncertainty of demand. It begins with a machine learning (ML) algorithm for contagion level prediction, which adjusts demand forecasts accordingly. Subsequently, the URSP approach incorporates risk aversion and various types of uncertainty by combining stochastic programming and robust optimization through an adjustable weight in the objective function. As a risk-aversion technique, conditional value-at-risk (CVaR) is employed to restrict shortage levels, providing a more realistic assessment of MSC resilience. To balance cost-effectiveness and robustness against a spectrum of uncertainties, the URSP method leverages the strengths of both stochastic programming and robust optimization. Taguchi's orthogonal array design is utilized to generate cases representing combinations of government policies aimed at mitigating potential risks during future epidemics or pandemics. The effectiveness of the proposed methodology is demonstrated through a comprehensive case study conducted in Türkiye, comparing several modeling approaches. Extensive experiments under different types of uncertainties are performed to assess MSC viability. Computational analysis reveals that the URSP approach provides more robust and computationally tractable solutions than the purely stochastic approach and offers more cost-effective kit allocation decisions than the purely robust approach by allowing decision-makers to fine-tune the robustness level based on their priorities. The insights indicate that integrating ML predictions with URSP significantly enhances MSC viability to withstand deep uncertainties during pandemics.

1. Introduction

The global COVID-19 pandemic has given rise to many major disruptions leading numerous risks for medical supply chains (MSCs), including: (i) a radical increase in the demand for essential medical supplies, (ii) a sharp rise in patient numbers, (iii) fluctuations in medical center capacity, and (iv) inefficiencies in the distribution of supplies [74]. These disruptions have presented numerous risks for MSCs. To mitigate the impact of pandemic-related risks, supply chain (SC) resilience has been considered from various angles, including design, resource utilization, distribution, and inventory management [26]. The resilience of an MSC is characterized by its ability to withstand disruptions, absorb shocks, adapt to changes, and recover performance, ensuring sustained functionality and a quick return to normal operations [21,66]. It involves both short-term recovery and long-term adaptation in response to disruptions under known-unknown uncertainty [44,64].

Known-unknown uncertainties refer to situations where some historical data or prior knowledge is available, but future outcomes cannot be determined with certainty. For example, while seasonal demand fluctuations for medical supplies can be estimated using historical usage patterns, the exact demand in the upcoming period remains uncertain. Such uncertainties are often represented using probability distributions

☆ Area: Data-Driven Analytics. This manuscript was processed by Associate Editor Prof. Benjamin Lev

* Corresponding author at: Department of Industrial Engineering, Karadeniz Technical University, Trabzon 61080, Turkey.
E-mail addresses: omerfarukyilmaz@ktu.edu.tr, omeryilmaz@ufl.edu (Ö.F. Yılmaz).

https://doi.org/10.1016/j.omega.2024.103264
Received 25 July 2024; Accepted 18 December 2024
Available online 24 December 2024
0305-0483/© 2024 Elsevier Ltd. All rights are reserved, including those for text and data mining, AI training, and similar technologies.

derived from the available data. In contrast, unknown-unknown uncertainties stem from events or conditions that are entirely novel and lack any historical precedent or reference point. A sudden outbreak of a previously unknown pathogen exemplifies this type of uncertainty, where neither its likelihood nor its impact can be easily quantified due to the absence of prior experience or data [51,76].

Being such a complex and dynamic network, MSCs have been frequently exposed to disruptions during the recent global pandemic. These disruptions, marked by severe shortages, revealed that traditional resilience plans are inadequate for ensuring industry survival in the post-pandemic era [23]. Since conventional disruption mitigation measures have proven insufficient for helping MSC networks navigate extremely volatile and uncertain environments, there is a strong need to address unknown-unknown uncertainties to ensure long-term survivability. This realization has led to the emergence of the concept of 'SC viability' in the face of black swan events [31].

Viability introduces a new approach to managing disruptions within SCs, distinctly different from the traditional focus on stability-based resilience [27]. Defined by Ivanov [24] as the ability to sustain and adapt in an evolving environment despite long-term impacts, SC viability centers on the concept of structural reconfiguration under unknown-unknown uncertainty [68]. This perspective emphasizes not just recovery from disruptions, but also the SC's ability to thrive in a dynamic environment over extended periods [28,61,65]. To achieve viability, SCs must undergo strategic restructuring and replanning to maintain long-term economic performance. This involves making critical adjustments to their structure, processes, and operations, ensuring they remain relevant and successful amidst evolving challenges [32,67].

The pandemic and post-pandemic era have underscored the importance of SC viability [43]. Existing models often fail to predict the severe impacts of disruptions because they do not fully account for the contagion effects of viruses [76]. While initial demand during the early stages of pandemic-induced disruptions can be represented by known unknown or unknown uncertainties, the highly transmissible nature of diseases often leads to ripple effects that overwhelm networks and hinder their ability to meet the demand for critical supplies [6]. Consequently, many MSCs struggle to sustain medical needs over the long term. Given these challenges, it is crucial to incorporate uncertainty through stochastic or robust optimization approaches, while also accounting for the contagion potential of diseases that directly affect medical product demand when designing resilient MSCs.

In traditional stochastic optimization, it is typically assumed that uncertain demand follows a specific probability distribution based on its best fit to historical data [78]. However, in real-world applications, relying on such a distribution can introduce bias due to the limited availability of historical data, potentially leading to suboptimal solutions [76]. Alternatively, robust optimization offers a different approach that requires less reliance on historical data. Instead of depending on a probability distribution, robust optimization defines an uncertainty set, which can be derived from limited data or even expert knowledge in the absence of historical information [51]. While this method enhances system robustness by focusing on minimizing the worst-case cost or regret, it often results in more conservative solutions, sacrificing cost-effectiveness to ensure reliability across all potential scenarios. However, this approach faces challenges due to its inherent over-conservatism, as minimizing worst-case costs can result in overly cautious strategies, especially since worst-case scenarios occur rarely. Thus, while stochastic optimization is more data-driven and can be biased when data is scarce, robust optimization prioritizes system resilience at the expense of cost-effectiveness. To address the limitations of both stochastic and robust optimization approaches, an innovative unified robust stochastic programming (URSP) approach is introduced, which leverages the strengths of both methods, particularly when historical data is available.

Motivated by the needs outlined above, this study proposes a comprehensive methodology that integrates machine learning (ML) with URSP to ensure MSC viability by addressing the medical kit allocation problem. The modeling approach evaluates demand from two perspectives: (i) known-unknown uncertainty through SP and (ii) unknown-unknown uncertainty, such as black swan events, through RO. In this unified framework, viability is assessed by the level of unsatisfied demand under uncertainty following day-ahead decisions. By accounting for these unknown-unknown uncertainties, the unified approach enhances both the reliability and applicability of the results, thereby ensuring MSC viability from the operational standpoint. The methodology begins with an ML algorithm to predict the contagion level of potential diseases that might lead to a pandemic and cause a ripple effect. Following this, optimization models are formulated to incorporate sustainability from an overall cost perspective in the objective function, while resilience is addressed by controlling the shortage level of supplies via the conditional value at risk (CVaR) approach in the constraints. Consequently, the proposed methodology is well-suited for solving the medical kit allocation problem by mitigating risks associated with both disruptions and ripple effects.

In the post-pandemic era, understanding the dynamics of MSC viability is crucial for mitigating the risks of future disruptions. Accordingly, this study aims to address the following research questions concerning MSC viability under both known-unknown and unknown-unknown uncertainty:

By implementing the proposed methodology, the following research questions are addressed in detail:

- **RQ-1:** Which optimization method, namely stochastic, robust, or combined, should be preferred to achieve MSC viability with respect to several performance metrics?
- **RQ-2:** How do risk aversion approaches affect system performance with respect to sustainability and resilience in the medical kit allocation problem?
- **RQ-3:** Which government policy implementations, represented by controllable factors and their levels, are most effective for MSC viability considering contagion levels?
- **RQ-4:** How does the structure of uncertainty affect the overall cost across the multiple optimization models?

The key contributions of this study to the field are outlined below.

- This study addresses the medical kit allocation problem within the MSC network by anticipating potential future disruptions in the post-COVID era. By incorporating contagion level predictions of diseases, it combines ML algorithms with a novel URSP approach within the context of MSC viability. The emphasis is on sustainability and resilience from an operational standpoint rather than a structural (re)design perspective. Accordingly, a new equation to compute contagion index (CI) has been developed.
- From a managerial standpoint, Taguchi's orthogonal array is employed to generate cases, each corresponding to a combination of government policies for Türkiye. Extensive experiments are conducted using multiple modeling approaches under different types of deep uncertainties to provide managerial insights and key findings on ensuring MSC viability and mitigating potential risks in the event of an epidemic or pandemic. Additionally, the modeling approaches are applied under various parameter settings for sensitivity analysis, allowing observation of the impact of risk aversion levels and disruption severity on MSC viability.
- From a methodological perspective, a comprehensive methodology beginning with an ML algorithm for contagion level prediction is developed to construct a set of modeling approaches that consider risk aversion and uncertainty types within the context of MSC viability. In these modeling approaches, risk aversion is incorporated through either RO, CVaR method, or both for comparison purposes. This allows for the identification of the most effective methods for

controlling maximum allowable shortage levels, ensuring a veneer of normalcy.

The rest of the study is organized as follows. Section 2 provides a detailed literature review, including a review table that highlights the differences between this study and previous studies in the existing literature. Section 3 presents the optimization model along with the proposed methodology. Computational analysis is detailed in Section 4, while discussions and managerial insights are provided in Section 5 to address the research questions. Finally, Section 6 offers concluding remarks on the study.

2. Literature review

This section provides an in-depth review of the existing literature on SC viability, aiming to develop a comprehensive framework that captures its key principles and dimensions. The discussion transitions to focus specifically on MSCs, where the unique challenges and requirements of these systems are explored. A critical analysis is presented, highlighting the strategies and methodologies proposed to enhance MSC viability while addressing interconnected aspects of resilience, robustness, and sustainability. This dual approach ensures a holistic understanding of both general SC viability and its specialized application to MSCs.

2.1. Supply chain viability

The COVID-19 pandemic exposed unprecedented uncertainties and vulnerabilities in SC, creating new challenges and disruptions that existing frameworks struggled to address [52,55]. Therefore, a comprehensive approach is required to ensure the survivability and adaptability of SCs in the face of long-term disruptions. [10,30]. In response, Ivanov [24] introduced the new concept of viability against disruptions, examining its relationships with robustness, resilience, agility, and sustainability through a proposed viable SC framework. Following this, several studies have investigated viability and highlighted the importance of implementing risk mitigation strategies to enhance SC viability [2,29]. For instance, Liu et al. [44] proposed an optimization approach to minimize disruption risks and improve SC viability. Sardesaia and Klingebiel [63] developed a methodology that quantitatively analyzes the effectiveness and efficiency of SC reconfigurations to maintain viability in the face of disruptions. Ivanov [25] introduced a framework employing an intelligent digital twin to stress-test SCs, highlighting its potential to enhance resilience and viability. Petrudi et al. [53] constructed a structural model to identify critical factors essential for maintaining viability. Ivanov [26] proposed an immune system-inspired mechanism approach, identifying potential research themes that could enhance SC resilience and viability. Sawik and Sawik [68] formulated a two-stage stochastic optimization model by incorporating the CVaR approach to ensure risk-averse viability and improve resilience under severe disruptions. Echefaj et al. [11] designed a simulation model to assess disruptions impacts and evaluate strategies for building resilient and viable SCs. These studies collectively demonstrate that organizations can effectively manage disruptions, sustain critical operations, and protect long-term sustainability by implementing strategies to improve SC viability.

2.2. Viability for MSCs

Despite significant advancements in exploring SC viability across various sectors, the healthcare industry faces unique challenges due to its critical demands [9]. Unlike general SCs, MSCs must ensure the continuous availability of essential items, such as life-saving equipment, vaccines, and medications, during prolonged disruptions [76]. Therefore, proactive strategies are crucial to effectively address disruptions in MSCs. Before the pandemic, research primarily concentrated on applying robust, resilient, and sustainable strategies to mitigate these disruptions [18,56]. For instance, Pishvaee et al. [54] developed a multi-objective possibilistic programming model for MSC network design, considering economic, environmental, and social dimensions of sustainability. Hasani and Khosrojerdi [19] devised an optimization model for designing a robust MSC network by integrating resilience strategies. To solve this problem, they utilized a parallel memetic algorithm. Fahimnia et al. [14] developed a stochastic optimization model for the blood SC network design problem under disaster uncertainty, aiming to minimize total costs. They employed the ε-constraint and Lagrangian relaxation method to solve the problem and bolster SC resilience. Sabouhi et al. [62] investigated the MSC design problem under operational and disruption risks taking into account quantity discounts. They developed a two-stage possibilistic-stochastic programming model to handle known-unknown uncertainty and improve SC resilience. Ma et al. [47] explored quality management in MSC by considering patient concerns to enhance SC sustainability and profitability. Kargar et al. [35] proposed a robust possibilistic programming model for designing a medical waste reverse supply chain under known-unknown uncertainty. Their study demonstrates the model's potential to enhance SC sustainability through a real case study. Goodarzian et al. [17] developed an optimization model addressing the distribution and location problem for a sustainable MSC, especially for COVID-19-related medicines with perishability concerns. Three hybrid meta-heuristic algorithms were employed to solve the addressed problem. Hasani et al. [20] introduced a multi-objective robust optimization model for designing the MSC network under disruption. They utilized a novel hybrid meta-heuristic algorithm to tackle this problem. This approach integrates budget uncertainty and risk mitigation strategies to enhance the sustainability and resilience of the SC. Ahmadi et al. [1] studied the location and allocation problem in emerging medical center SC, aiming to improve resilience and accessibility. Gilani and Sahebi [16] developed a data-driven robust optimization model for a sustainable COVID-19 vaccine SC, ensuring efficient distribution both domestically and internationally. Karadayi-Usta and Serdarasan [34] suggested fuzzy rule-based inference system approach for supplier selection and order allocation problem in sustainable medical tourism SC. Wang et al. [73] formulated a robust optimization model for the distribution problem in vaccine SC under supply uncertainty. Nayeri et al. [50] addressed the order allocation and supplier selection problem for MSC by considering responsiveness, sustainability, and resilience aspects simultaneously. They proposed data-driven based model and employed Chebyshev multi-choice goal programming approach to solve the problem. Alizadeh et al. [3] presented a scenario-based two-stage stochastic programming approach to configure the MSC structure for the post-pandemic era. They utilized the benders decomposition algorithm to solve the addressed problem. Li et al. [42] proposed a multi-objective mixed-integer nonlinear programming model for medical supply distribution and resource allocation problem to enhance the SC sustainability. Kar et al. [33] utilized ML approach to predict the quantities of medical supplies and the actual delivery days in healthcare SCs. They also proposed strategies for risk management and improving the robustness of the SC.

These contributions highlight the critical role of MSCs in building sustainable, robust, and resilient healthcare systems. However, the pandemic underscored the necessity for frameworks that extend beyond mere resilience and robustness to address unknown-unknown uncertainties and unprecedented disruptions [60]. Therefore, it is imperative to develop comprehensive strategies that render MSCs viable, resilient, and sustainable across multiple dimensions. In this regard, recent studies have begun exploring solutions to enhance viability and resilience within MSCs during crises. For instance, Alizadeh et al. [4] investigated a viable healthcare network design problem through a real case study conducted during the COVID-19 pandemic disruption. They proposed a multi-stage stochastic optimization model with the objectives of maximizing patient recovery and minimizing costs and mortality

rates under conditions of known-unknown uncertainty. Hussaini et al. [22] devised a mixed-integer mathematical model to examine various resilience and viability strategies in response to demand fluctuations in MSC planning. They employed an optimal grading method to solve a real case problem. Zaoui et al. [77], dealt with forecasting problem within the MSC for predicts vaccine deliveries and vaccination rates. They utilized ML algorithm to supporting SC resilience, ensuring the viability, and managing risk during a pandemic crisis. Lotfi et al. [46] studied the network design problem in MSC by considering resilience and viability requirements. A two-stage robust stochastic programming approach combined with a weighted value at risk method was employed to improve the SC's viability, robustness, and risk aversion under known-unknown uncertainty.

While numerous risk mitigation and aversion strategies are suggested in the literature to strengthen the resilience, sustainability, and robustness of MSC in the face of disruptions, there are few instances of employing CVaR method. Xie et al. [74] developed a mathematical model for designing an emergency MSC within the framework of corporate social responsibility and government subsidies. They employed CVaR method as a risk measurement criterion to mitigate risks and increase the sustainability of SC during the pandemic. Lotfi et al. [45] presented a two-stage robust stochastic optimization model for the MSC network design problem, considering viability, resilience, and robustness. They utilized the CVaR method to address risk aversion by restricting shortage levels. However, their study has several limitations. They only consider the worst-case scenario among the scenarios generated for the SP part. Additionally, they only address known-unknown uncertainties, as the uncertainty is solely represented through generated scenarios. Therefore, their approach is limited in addressing the MSC network design problem from a viability perspective due to the lack of consideration of unknown-unknown uncertainty.

2.3. Research gaps and contributions

Table 1 categorizes prior research on MSCs according to problem type, supply chain framework, uncertainty type, problem characteristics, and solution approaches, providing a clear overview of research gaps.

An analysis of the literature reveals that while many studies propose strategies to enhance MSC viability, most focus solely on known-unknown uncertainties, often in the context of network design, distribution planning, or supplier selection. However, there is limited research on allocation-specific problem in MSCs, which is critical for ensuring effective resource distribution, especially under uncertainty. Additionally, much of the current literature lacks comprehensive approaches that address MSC viability, resilience, robustness, and sustainability when unknown-unknown uncertainties arise. Furthermore, a shortage of studies that integrate ML algorithms with optimization methods to predict and manage evolving uncertainties is evident. To address these gaps, this study addresses the medical kit allocation problem with a focus on MSC viability from an operational perspective. Our model represents the randomness of the uncertain parameters in the

Table 1
Previous studies on MSCs.

Author	Problem Type	SC Framework				Uncertainty Type	**Problem Characteristics**			**RCS**	**Solution Methods**
		V	RE	S	RO		**D**	**RA**	**CVaR**		
Pishvaee et al. [54]	MSC Network design			*	*	Known-Unknown		*		*	PP and BDA
Hasani and Khosrojerdi [19]	MSC Network design		*		*	Known-Unknown	*	*		*	PMA and LRM
Fahimnia et al. [14]	MSC Network design		*			Known-Unknown	*				ε-constraint and LRM
Ramezanian and Behboodi [56]	MSC Location-allocation		*		*	Known-Unknown		*		*	ROP
Sabouhi et al. [62]	MSC Network design		*			Known-Unknown	*	*		*	TPSP
Ma et al. [47]	MSC Decision making			*		Deterministic				*	SGA
Kargar et al. [35]	MSC Network design			*	*	Known-Unknown		*		*	FGP and RPP
Goodarzian et al. [17]	MSC Distribution-location			*	*	Known-Known				*	SOM and HMH
Hasani et al. [20]	MSC Network design		*			Known-Unknown	*	*		*	OM and HMH
Ahmadi et al. [1]	MSC Network design		*			Deterministic	*	*		*	ACO and QAPM
Gilani and Sahebi [16]	MSC Distribution planning			*	*	Known-Unknown		*		*	ROP
Lotfi et al. [45]	MSC Network design	*	*	*	*	Known-Unknown	*	*	*	*	TRSP
Yılmaz et al. [76]	MSC Network design		*		*	Known-Unknown	*	*		*	TSP and LM
Alizadeh et al. [4]	MSC Network design	*				Known-Unknown	*	*		*	MSP
Xie et al. [74]	MSC Network design			*		Known-Known	*	*	*		OM
Han et al. [18]	MSC Allocation				*	Deterministic				*	OM and HMH
Hussaini et al. [22]	MSC Supplier selection	*	*	*		Deterministic	*				OM
Wang et al. [73]	MSC Distribution-location				*	Known-Known		*		*	TROP
Nayeri et al. [50]	MSC Allocation and supplier selection		*	*		Known-Known	*			*	CMCGP-UF and MLA
Zaoui et al. [77]	MSC Forecasting	*	*			Known-Unknown	*	*		*	MLA
Karadayi-Usta and Serdarasan [34]	MSC Allocation and supplier selection			*		Known-Known				*	FRBIS
Alizadeh et al. [3]	MSC Network design		*	*		Deterministic	*	*			TSP and BDA
Lotfi et al. [46]	MSC Network design	*	*	*	*	Known-Unknown	*	*		*	TRSP
Li et al. [42]	MSC Location-allocation			*		Deterministic		*			OM and ε-constraint
Kar et al. [33]	MSC Forecasting				*	Deterministic		*			MLA
This Study	**MSC Allocation**	*	*	*	*	Unknown-Unknown, Known-Unknown	*	*	*	*	**URSP and MLA**

SC: Supply Chain, V: Viability, RE: Resilience, S: Sustainability, RO: Robustness, D: Disruption, RA: Risk Aversion, RCS: Real case study, CVaR: Conditional value-at-risk, RPP: Robust possibilistic programming, FGP: Fuzzy goal programming, PP: Possibilistic programming, BDA: Benders decomposition algorithm, LRM: Lagrangian relaxation methods, PMA: Parallel memetic algorithm, ROP: Robust optimization programming, OM: Optimization model, TPSP: Two-stage possibilistic-stochastic programming, SGA: Stackelberg game approach SOM: Simulation optimization model, FRBIS: Fuzzy rule-based inference system HMH: Hybrid meta-heuristic, ACO: Ant colony optimization, QAPM: Quadratic assignment problem methods, ECBO: Enhanced colliding bodies TRSP: Two-stage robust stochastic programming, LM: Lean management, TSP: Two-stage stochastic optimization, MSP: Multi-stage stochastic programming, TROP: Two-stage robust optimization programming, CMCGP-UF: Chebyshev Multi-Choice Goal Programming with Utility Function, MLA: Machine learning algorithm, URSP: Unified Robust Stochastic Programming.

SP part using a finite probability space with probabilities p^s. Additionally, we consider an uncertainty interval for the RO part that is independent of the SP scenarios. The common decision made for both RO and SP parts is the day-ahead allocation, which is directly influenced by the level of robustness introduced in our model. This allows our model to address both known-unknown and unknown-unknown uncertainties. Since viability can only be ensured by accounting for unknown-unknown uncertainties, this study effectively addresses viability from an operational aspect. Furthermore, we propose a comprehensive methodology that combines ML algorithms with the URSP model. Using ML techniques -namely Random Forest (RF), Gradient Boosting (GB), and K-Nearest Neighbors (KNN)-, we predict the contagion levels of diseases and represent their impact on demand through the URSP model. The impact of using CVaR and RO as risk-averse techniques to handle extreme demand fluctuations and potential shortages is also investigated in the study. By applying the proposed methodology to a real case study, significant improvements in MSC viability are demonstrated, showing how the combined approach effectively enhances viability under unknown-unknown uncertainty. Critical insights into the role of allocation strategies within MSCs are provided by this approach, particularly in dynamically adjusting resource allocation to meet fluctuating demand during disruptions.

3. Optimization model and proposed methodology

This study examines the medical kit allocation problem within the context of MSC viability by considering the extensive demand increases experienced by MSC during disruptions such as the recent global COVID-19 pandemic. To overcome these challenges, the study suggests integrating ML algorithms with a URSP approach. The problem statement is followed by the proposed methodology to address this issue effectively.

Formally, the addressed problem can be stated as follows: there are sets of I and S related to hospitals and scenarios, respectively. The objective is to fulfill the standardized medical kit requirements of hospitals during the pandemic. To achieve this, medical kits are initially transported from a medical supplier to a medical warehouse. If needed, suppliers produce additional kits to meet the demand by considering day-ahead decisions. Both production and transportation costs are considered to supply multiple hospitals with medical kits from the medical warehouse. The primary goal is to obtain a medical kit allocation plan that minimizes the total operational cost for the sake of sustainability during a pandemic. The addressed medical kit allocation problem is illustrated with a schematic representation in Fig. 1.

Existing literature has explored both robust optimization and two-stage stochastic programming formulations to make day-ahead and second-stage decisions for the medical kit allocation problem. However, each approach has specific limitations: the stochastic optimization approach faces computational challenges due to large scenario sizes, while the robust optimization approach tends to be overly conservative [79]. In this study, we propose a novel URSP model that combines the strengths of both approaches. This model is designed to achieve a low expected total cost while ensuring system robustness. By introducing adjustable weights for the stochastic and robust components in the objective function, decision-makers can tailor the model based on their preferences. Since viability requires consideration of unknown-unknown uncertainties, the proposed modeling approach effectively addresses MSC viability as long as the decision-makers' preferences for the level of robustness (Γ) are set between 0 and 1.

The URSP model is formulated under the following assumptions:

- The disruption is considered only for the increases in demand at the hospitals.
- The medical kit allocation plan is made for a single planning period.
- There is a standard single medical kit available.

3.1. Proposed unified robust stochastic programming approach

In this section, the proposed URSP model is constructed to make day-ahead and second-stage decisions regarding the medical kit allocation problem.

Sets

I	Set of hospitals, indexed by i and j $\{i,j \in I\}$
S	Set of scenarios, indexed by s $\{s \in S\}$

Parameters

I_0	the initial inventory level for medical kit
t_i	the transportation cost of one unit of kit from medical warehouse to the hospital i
p	the production cost of one unit of kit (including transportation cost from supplier to warehouse)

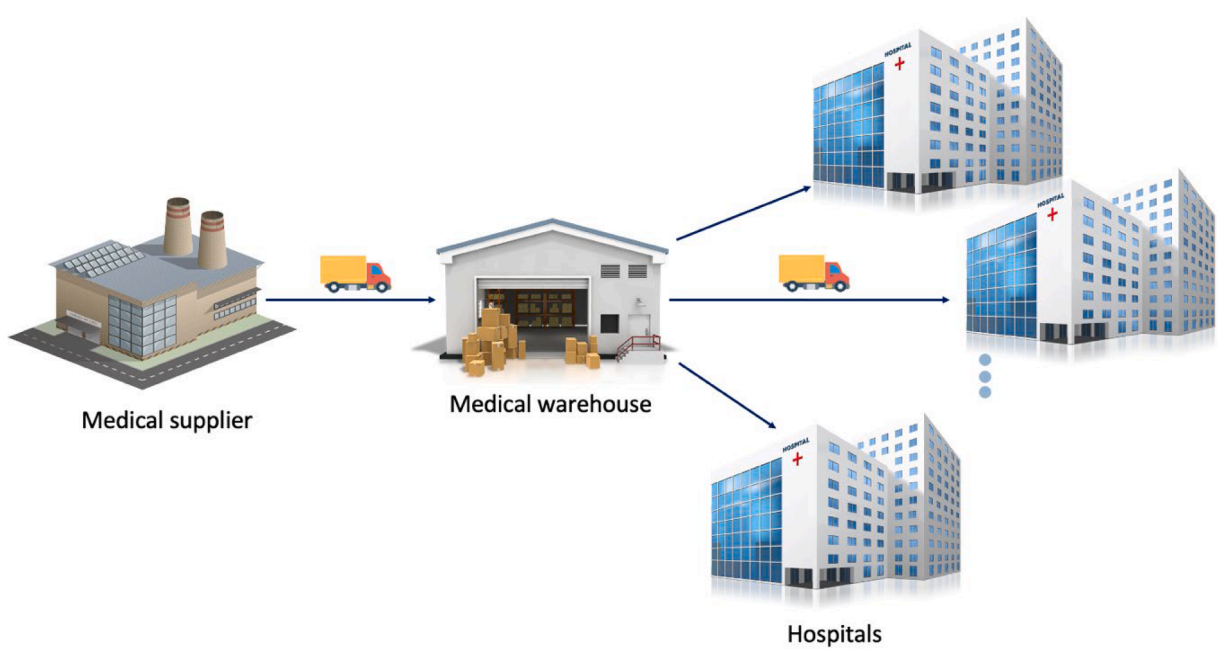

Fig. 1. The schematic representation of the problem.

C the production capacity
φ_i the CI of hospital i associated with the relevant district
$d_i(x,\xi)$ the demand of the hospital i when ξ is realized
$\mathscr{d}_i(x,\mathscr{d})$ the demand of the hospital i for the RO part
Γ the level of robustness, i.e., weight of objectives

Decision variable for the first stage:

x_i the amount of medical kits allocated to the hospital i

Decision variables for the second stage:

$y_i(x,\xi)$ the amount of kits produced for the hospital i when ξ is realized
$\phi_i(x,\mathscr{d})$ the amount of kits produced for the hospital i for the RO part

Dependent variables for the second stage:

$h_i(x,\xi)$ the amount of surplus inventory at the hospital i when ξ is realized
$\mathscr{B}_i(x,\xi)$ the amount of unsatisfied demand at the hospital i when ξ is realized
$\delta_i(x,\xi)$ the percentage of unsatisfied demand at the hospital i when ξ is realized
$\varpi_i(x,\mathscr{d})$ the amount of surplus inventory at the hospital i for the RO part
$\tau_i(x,\mathscr{d})$ the amount of unsatisfied demand at the hospital i for the RO part
$\zeta_i(x,\mathscr{d})$ the percentage of unsatisfied demand at the hospital i for the RO part

The first-stage problem:

$$z = \min \sum_{i\in I} t_i x_i + (1-\Gamma)\mathscr{C}(x,\xi) + \Gamma \max_{\mathscr{d}\in\mathscr{D}} \min_{\phi\in\Theta(x,\mathscr{d})} \sum_{i\in I}((t_i+p)\phi_i(x,\mathscr{d}) + \mathscr{g}\tau_i(x,\mathscr{d}) + \hbar\varpi_i(x,\mathscr{d})) \tag{1}$$

s.t

$$\sum_{i\in I} x_i \le I_0 \tag{2}$$

$$x_i \ge 0 \forall i \in I \tag{3}$$

The second-stage problem:

$$\mathscr{C}(x,\xi) = \min \sum_{i\in I}((t_i+p)y_i(x,\xi) + \mathscr{g}\mathscr{B}_i(x,\xi) + \hbar h_i(x,\xi)) \tag{4}$$

s.t

$$x_i + y_i(x,\xi) - h_i(x,\xi) + \mathscr{B}_i(x,\xi) = d_i(x,\xi)\varphi_i \forall i \in I \tag{5}$$

$$\sum_{i\in I} y_i(x,\xi) \le C \tag{6}$$

$$y_i(x,\xi) \ge 0 \forall i \in I \tag{7}$$

$$h_i(x,\xi) \ge 0 \forall i \in I \tag{8}$$

$$\mathscr{B}_i(x,\xi) \ge 0 \forall i \in I \tag{9}$$

and

$$\Theta(x,\mathscr{d}) = \{\phi :$$

$$x_i + \phi_i(x,\mathscr{d}) - \varpi_i(x,\mathscr{d}) + \tau_i(x,\mathscr{d}) = \mathscr{d}_i(x,\mathscr{d})\varphi_i \forall i \in I \tag{10}$$

$$\sum_{i\in I} \phi_i(x,\mathscr{d}) \le C \tag{11}$$

$$\phi_i(x,\mathscr{d}) \ge 0 \forall i \in I \tag{12}$$

$$\varpi_i(x,\mathscr{d}) \ge 0 \forall i \in I \tag{13}$$

$$\tau_i(x,\mathscr{d}) \ge 0 \forall i \in I\}. \tag{14}$$

In the proposed model, we introduce a level of robustness parameter (Γ), which assigns a weight to the expected total cost and the worst-case cost in the objective function. This allows system operators to adjust the importance of each objective according to their preferences [79]. When Γ is set to zero, the model reduces to a two-stage stochastic optimization problem, with additional constraints generated from the robust optimization approach. Conversely, when Γ equals one, the model focuses solely on the worst-case cost. The proposed URSP approach leverages the strengths of both stochastic and robust optimization, providing medical kit allocation decisions that minimize the expected total cost while ensuring system robustness. This results in less conservative solutions than the two-stage robust optimization method, while offering more robust solutions than the two-stage stochastic optimization approach [78].

In the two-stage formulation, the first stage determines allocation decisions, such as the amount of medical kits to allocate to each hospital. The second stage involves decisions on kit production for each hospital, accounting for different scenarios in the stochastic optimization part and the worst-case scenario in the robust optimization part. By adjusting the Γ parameter, decision-makers can control the balance between minimizing expected costs and preparing for the worst-case scenario.

The following parameters and variables are defined to obtain extensive form of the problem with CVaR constraints.

Parameters

p^s the probability associated with the scenario s
d_i^s the demand of the hospital i for the scenario s
α the confidence level for CVaR ($\alpha = 0$ means risk neutral case)
ϵ the upper bound for the CVaR of shortages
Δ the robust parameter to describe the uncertainty set
$\mathscr{g}$ the backorder cost
$\hbar$ the holding cost

Decision variables

y_i^s the amount of kits produced for the hospital i when the scenario s occurs
ϕ_i the amount of kits produced for the hospital i for the RO part

Dependent variables

h_i^s the amount of surplus inventory at the hospital i when the scenario s occurs
$\mathscr{B}_i^s$ the amount of unsatisfied demand at the hospital i when the scenario s occurs
$\delta_i{}^s$ the percentage of unsatisfied demand at the hospital i when the scenario s occurs
ϖ_i the amount of surplus inventory at the hospital i for the RO part
τ_i the amount of unsatisfied demand at the hospital i for the RO part
ζ_i the percentage of unsatisfied demand at the hospital i for the RO part
η VaRof unsatisfied demand at the confidence level α for the SP part
w^s the excess of maximum shortage percentage for the scenario s with respect η for the SP part
ν the excess of maximum shortage percentage for the scenario s with respect η for the robust optimization part
ς VaR of unsatisfied demand at the confidence level α for the RO part
Λ_i auxiliary variable defined for the RO part
λ_i auxiliary variable defined for the RO part

In this form, the randomness of the uncertain parameters is represented by a finite probability space with p^s. To quantify risks beyond value-at-risk (VaR), conditional value-at-risk (CVaR) is preferred as it captures a wider range of risk preferences [36]. This study examines how CVaR and robust optimization function both collaboratively and independently as approaches to risk aversion.

CVaR is employed to manage unsatisfied demand (restricted shortages) within the medical kit allocation problem, encompassing both

allocation decisions in the first stage and production decisions in the second stage. When disruptions occur at a ripple effect scale, considering only unmet demand in the objective function can lead to biased outcomes. For instance, if the cost of unsatisfied demand increases significantly due to the ripple effect, suppliers may prioritize meeting all demand regardless of cost. Conversely, given the urgent nature of medical supplies during outbreaks, it is unrealistic to assume that the cost of unmet demand would be low. Therefore, implementing the CVaR approach helps to restrict shortages and provides a more realistic assessment of MSC performance in terms of resilience under uncertainty.

The classical linear programming representation of CVaR at the confidence level α, for random variable Ξ with realizations ξ^s, $s \in S$, and corresponding probabilities p^s, $s \in S$, is given by [36,59].

$$\mathrm{CVaR}_\alpha(\Xi) = \min\left\{\eta + \frac{1}{1-\alpha}\sum_{s\in S} p^s w^s \ : \ w^s \geq \xi^s - \eta \ \forall s \in S, \ w \in \mathbb{R}_+^{|S|}, \ \eta \in \mathbb{R}\right\} \tag{15}$$

where η is the value at risk at confidence level α, which is represented by $\mathrm{VaR}_\alpha(\Xi)$. The variable w correspond to the larger values than $\mathrm{VaR}_\alpha(\Xi)$. It can be stated that CVaR_α for a random variable is computed by weighted sum of excess values with respect to $\mathrm{VaR}_\alpha(\Xi)$.

For a threshold value $\epsilon \in \mathbb{R}$, the inequality $\mathrm{CVaR}_\alpha(\Xi) \leq \epsilon$ holds if and only if there exist $w \in \mathbb{R}^{|S|}$ and $\eta \in \mathbb{R}$ satisfying [36,58,59]:

$$\eta + \frac{1}{1-\alpha}\sum_{s\in S} p^s w^s; \quad w^s \geq \xi^s - \eta \ \forall s \in S \tag{16}$$

Based on the linear programming formulation of CVaR presented above, the following decision variables are defined to consider the constraint $\mathrm{CVaR}_\alpha(\| \delta^s \|_\infty) \leq \epsilon$. w^s, $\bar{\delta}^s \geq 0$ for $s \in S$ and $\eta \geq 0$, and the following constraints are generated:

$$\eta + \frac{1}{1-\alpha}\sum_{s\in S} p^s w^s \leq \epsilon \tag{17}$$

$$w^s \geq \bar{\delta}^s - \eta \ \forall s \in S \tag{18}$$

$$\bar{\delta}^s \geq \delta_i^s \ \forall i \in I, \forall s \in S \tag{19}$$

$$w^s \geq 0 \ \forall s \in S \tag{20}$$

$$\bar{\delta}^s \geq 0 \ \forall s \in S \tag{21}$$

$$\eta \geq 0 \tag{22}$$

The decision variable $\bar{\delta}^s$ used to represent $\| \delta^s \|_\infty$ can be eliminated by changing $\bar{\delta}^s$ by δ_k^s for all $k \in K$:

$$\eta + \frac{1}{1-\alpha}\sum_{s\in S} p^s w^s \leq \epsilon \tag{23}$$

$$w^s \geq \delta_i^s - \eta \ \forall i \in I, \forall s \in S \tag{24}$$

$$w^s \geq 0 \ \forall s \in S \tag{25}$$

$$\eta \geq 0 \tag{26}$$

The reason for using CVaR as a risk measure is to limit the level of unsatisfied demand within the constraints. Since shortage and holding costs are not included in the objective function, neither in the SP parts nor in the RO part, CVaR constraints should be incorporated into the RO part. The following CVaR constraints are developed for this purpose.

$$\varsigma + \frac{1}{1-\alpha}\nu \leq \epsilon \tag{27}$$

$$\nu \geq \zeta_i - \varsigma \ \forall i \in I \tag{28}$$

$$\nu \geq 0 \tag{29}$$

$$\varsigma \geq 0 \tag{30}$$

In order to obtain the uncertainty set associated with the RO part, it is assumed that the demand of the ith hospital d_i vary between a lower bound d_i^- and upper bound d_i^+ which corresponds to the fifth and 95th percentile of the random demand. When the contagion impact is considered, the lower and upper bounds are revised as $d_i^- \varphi_i$ and $d_i^+ \varphi_i$ respectively.

$$\mathscr{D} := \{\mathscr{d} \in Z^{|I|} : \ \mathscr{d}_i^- \varphi_i \leq \mathscr{d}_i \leq \mathscr{d}_i^+ \varphi_i \ \forall i \in I \tag{31}$$

$$\sum_{i\in I} \mathscr{d}_i \leq C + I_0 \ \forall i \in I\} \tag{32}$$

In the optimization model, while the SP part is represented by a scenario-based approach, the RO part is represented by incorporating the sets $\mathscr{D}$ and $\Theta(x, \mathscr{d})$ into their equivalent constraint sets. Recall the Eq. (10):

$$x_i + \phi_i(x, \mathscr{d}) - \varpi_i(x, \mathscr{d}) + \tau_i(x, \mathscr{d}) = \mathscr{d}_i(x, \mathscr{d})\varphi_i \forall i \in I$$

From Eq. (10), we know that $\phi_i = \mathscr{d}_i\varphi_i - x_i + \varpi_i - \tau_i$. When we replace the ϕ_i in $\min_{\phi\in\Theta(x,\mathscr{d})} \sum_{i\in I}(t_i + p)\phi_i(x, \mathscr{d})$ in Eq. (1), we obtain the following RO part: $\Gamma \max_{\mathscr{d}\in\mathscr{D}} \mathscr{G}(x, \mathscr{d})$ where $\mathscr{G}(x, \mathscr{d}) = \sum_{i\in I}(t_i + p)(\mathscr{d}_i\varphi_i - x_i + \varpi_i - \tau_i)$. To integrate this equation into the optimization model, the new variable Λ_i is introduced such that $\Lambda_i \geq \mathscr{G}(x, \mathscr{d})$. It can also be derived that $\Lambda_i \geq \mathscr{G}(x, \mathscr{d}_i^+)$. Therefore, in the following optimization model, the RO part is derived from the upper bound of demand uncertainty interval.

The extensive form of the deterministic equivalent problem is formulated as follows:

$$z = \min \sum_{i\in I} t_i x_i + (1-\Gamma)\sum_{i\in I}\sum_{s\in S} p^s\left(y_i^s(t_i + p) + \mathscr{g}\mathscr{B}_i^s + \hbar h_i^s\right) + \Gamma\sum_{i\in I}((t_i + p)(\lambda_i) + \mathscr{g}\tau_i + \hbar\varpi_i) \tag{33}$$

s.t

$$\sum_{i\in I} x_i \leq I_0 \tag{34}$$

$$x_i + y_i^s - h_i^s + \mathscr{B}_i^s = d_i^s\varphi_i \forall i \in I, \ \forall s \in S \tag{35}$$

$$\sum_{i\in I} y_i^s \leq C \forall s \in S \tag{36}$$

$$\delta_i^s = \mathscr{B}_i^s / d_i^s\varphi_i \ \forall i \in I, \ \forall s \in S \tag{37}$$

$$\eta + \frac{1}{1-\alpha}\sum_{s\in S} p^s w^s \leq \epsilon \tag{38}$$

$$w^s \geq \delta_i^s - \eta \ \forall s \in S \tag{39}$$

$$w^s \geq 0 \ \forall s \in S \tag{40}$$

$$\eta \geq 0 \tag{41}$$

$$\delta_i^s \geq 0 \tag{42}$$

$$\lambda_i \geq \mathscr{d}_i^+\varphi_i - x_i + \varpi_i - \tau_i \ \forall i \in I \tag{43}$$

$$\sum_{i\in I} \lambda_i \leq C \tag{44}$$

$$\zeta_i = \tau_i / \mathscr{A}_i^+ \varphi_i \ \forall i \in I, \ \forall s \in S \tag{45}$$

$$\varsigma + \frac{1}{1-\alpha}\nu \leq \epsilon \tag{46}$$

$$\nu \geq \zeta_i - \varsigma \ \forall i \in I \tag{47}$$

$$\nu \geq 0 \tag{48}$$

$$\varsigma \geq 0 \tag{49}$$

$$\zeta_i \geq 0 \tag{50}$$

$$y_i^s \geq 0 \text{ and integer } \forall i \in I, \ \forall s \in S \tag{51}$$

$$h_i^s \geq 0 \text{ and integer} \forall i \in I, \ \forall s \in S \tag{52}$$

$$\mathscr{B}_i^s \geq 0 \text{ and integer} \forall i \in I, \ \forall s \in S \tag{53}$$

$$x_i \geq 0 \text{ and integer} \forall i \in I \tag{54}$$

$$\varpi_i \geq 0 \text{ and integer } \forall i \in I \tag{55}$$

$$\tau_i \geq 0 \text{ and integer} \forall i \in I \tag{56}$$

$$\lambda_i \geq 0 \text{ and integer } \forall i \in I \tag{57}$$

The proposed URSP model is a novel integration that combines elements of both SP and RO to address different types of uncertainties. In this URSP model, known-unknown uncertainties are addressed through the SP component, while unknown-unknown uncertainties are managed using the RO component. The model assesses MSC viability from an operational perspective by measuring the amount of unsatisfied demand.

The objective function (33) minimizes the overall operational cost consisting of transportation, production, backorder and holding inventory costs regarding both SP and RO parts. Constraint (34) ensures that the amount of medical kits allocated to the hospital i cannot be exceed the initial inventory level in the first stage, before the realization of uncertainty. After the realization of uncertainty, Constraint (35) ensures the balance of demand, surplus inventory, unsatisfied demand, and the allocation of medical kits to hospital i for the SP part. Constraint (36) guarantees that the amount of kits produced for the hospital i in scenario s cannot exceed the production capacity. Constraint (37) is used to calculate the percentage of unsatisfied demand at hospital i when the uncertainty is realized for the SP part. Constraints (38)-(42) are related to the CVaR method to control the unsatisfied demand level. In this URSP model, setting $\alpha = 0$ corresponds to the risk-neutral case, while $\alpha = 1$ represents the worst-case scenario regarding unsatisfied demand for the specified product type. When $\epsilon = 1$, shortages are permitted for the relevant product type and only reflected in the objective function through. Conversely, setting $\epsilon = 0$ is means that shortages are not allowed.

Constraint (43) maintains the balance of demand, surplus inventory, amount of unsatisfied demand, and the allocation medical kits to the hospital i for the RO part. Constraint (44) guarantees that the amount of kits produced for the hospital i cannot exceed the production capacity for the RO part. Constraint (45) calculates the percentage of unsatisfied demand for the hospital i for the RO part. Constraints (46)-(50) relate to the CVaR approach for the RO part. The explanations provided for the CVaR parameters in the SP section are also applicable to the RO section. Constraints (51)-(53) represent day-ahead decisions, denoting the non-negativity restriction of the decision variables for the SP part. Constraints (54) indicates the nonnegativity restriction for the first stage decision variables. Constraints (55)-(57) are non-negativity restriction for the decision variables related to the RO part.

The SP and RO components share decision variables within the unified model, ensuring that allocations are optimized while considering both types of uncertainties concurrently. Solving the URSP model as a single entity allows for dynamic management of trade-offs between cost and robustness, rather than treating SP and RO in isolation, which could lead to conflicting decisions. The true day-ahead decision in the URSP model is derived from the optimized allocation that simultaneously satisfies the objectives of both SP and RO components, weighted according to the specified preferences. This integrated solution ensures that the MSC remains both cost-effective and resilient against a spectrum of uncertainties, rather than oscillating between purely cost-driven or purely robustness-driven decisions. Additionally, the second-stage decision variables corresponding to the SP and RO components are evaluated separately. Both sets of decision variables represent post-uncertainty situations following day-ahead decisions, with the RO component addressing the worst-case scenario and the SP component addressing the expected scenario. Therefore, they can be considered separately, and the results can be analyzed from this perspective.

3.2. Proposed methodology

This study proposes a methodology that integrates ML algorithms with an URSP approach to address the medical kit allocation problem in the post-COVID era. Initially, to estimate the CI, all districts within the relevant region are considered, and factors influencing the contagion level are identified. Subsequently, different strategic cases, each related to a combination of government policies, are realized by considering changes in legislation, higher education policies, and healthcare policies.

ML algorithms, including RF, GB, and KNN, are employed for regression prediction in each case. This approach estimates the CI values of an outbreak in any region of Türkiye during a potential pandemic. For each ML algorithm, a regression function is used, and the data is normalized to obtain the CI values.

Following that, the estimated CI values are used as parameters in the formulated URSP approach. To obtain detailed results and facilitate meaningful comparisons, an extensive computational analysis is carried out. This includes a Taguchi DoE setting with a detailed sensitivity analysis that evaluates various models, encompassing RO with and without CVaR approaches, SP with and without CVaR approaches, as well as hybrids that combine both robust and stochastic programming (URSP) with and without CVaR approaches. The flowchart of the proposed methodology is presented in Fig. 2. As illustrated in this figure, six different modeling approaches are considered in this study, each of which corresponds to a different set of constraints.

3.2.1. Machine learning techniques

In this section, the employed distinct ML algorithms for regression prediction are briefly explained.

i. **Random Forest (RF):** RF algorithm is an ensemble learning technique used for both classification and regression tasks. It constructs multiple decision trees during training and outputs the mean prediction for regression or the majority vote for classification [70]. This approach effectively reduces overfitting and improves model performance by averaging the predictions of numerous weak decision trees, thereby leveraging their complementarity to enhance overall decision accuracy [13]. RF is widely used in various fields, including energy, medical management, finance, and logistics [8,48] due to its robustness and versatility in handling large datasets and complex variable interactions.

ii. **Gradient Boosting (GB):** GB is a ML technique that enhances model performance by operating in a functional space, focusing on pseudo-residuals instead of the traditional residuals used in conventional boosting methods [38]. In regression tasks, GB constructs decision trees in a step-by-step manner, where each tree attempts to correct the prediction errors made by the

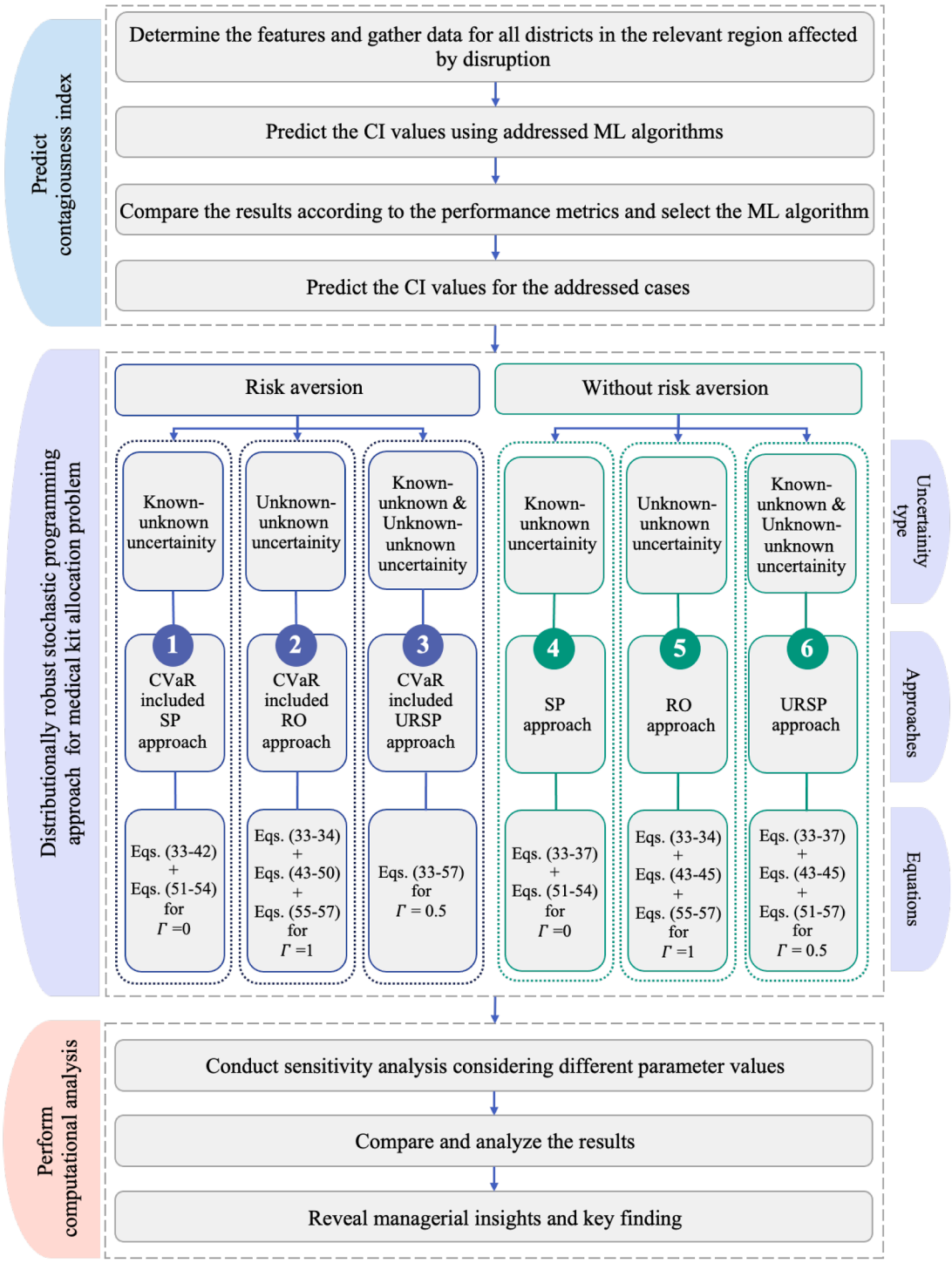

Fig. 2. The flow diagram of the proposed methodology.

previous trees. The final model is an ensemble of these trees, which together provide a robust prediction by averaging the outputs of all individual trees. This method effectively handles overfitting and enhances model performance by leveraging the strengths of multiple weak learners [5]. GB has been successfully applied in various fields including economics [15], energy [71], healthcare [69], and SC management [75].

iii. **K-Nearest Neighbors (KNN):** KNN is a simple, non-parametric algorithm used for classification and regression. It works by identifying the 'k' nearest data points to a given query point and making predictions based on the majority class (for classification) or the average value (for regression) of these neighbors [41]. KNN is widely applied in SC management, economics and finance, healthcare management, and energy management [39] due to its ease of implementation and effectiveness in straightforward relationships.

4. Computational analysis

4.1. Background of real application case

During the COVID-19 pandemic, the virus's high level of contagion

was one of its most critical impacts. This affected nearly all stakeholders in the MSC network, particularly disrupting essential services at demand points like hospitals, medical care centers, pharmacies, and local healthcare providers, ultimately endangering human lives. While suppliers and warehouses had previously prepared for pandemics caused by known diseases, they were not ready for COVID-19, which acted as a 'black swan' event, leading to devastating impacts on the MSC. The rapid spread of the virus meant that many critical needs could not be met. Given these circumstances, in the post-COVID era, it is vitally important to consider the potential impacts of future pandemics and prepare accordingly through robust MSC design.

To assess the impact of the contagion level of disease on the MSC, computational experiments are performed for Trabzon province, which is located in the northern region of Türkiye (i.e., Black Sea region). In this regard, three different policies, consisting of changes in legislation, higher education policies, and healthcare policies are examined by considering one supplier, one medical warehouse, and 22 hospitals in Trabzon. The addressed medical kit allocation problem is visualized in Fig. 3.

4.2. Experimental settings

In this study, the COVID-19 pandemic is conceptualized as a ripple effect that impacts all stages and stakeholders of the MSC. To establish a viable MSC, we combine ML to predict the CI, which also operates as an adjustment index, with a URSP model. The CI is designed to estimate the contagion level of a disease, enabling us to adjust demand levels based on expected contagion trends. Specifically, the predicted CI values are incorporated into the demand forecasts for medical kits, allowing the model to account for increased demand resulting from higher contagion. If there is no contagion risk, the CI value is zero, and demand remains unadjusted.

The CI, calculated as the average weekly rate of increase or decrease in infections, provides insight into contagion dynamics by reflecting whether infections are accelerating, stabilizing, or declining. This approach is based on the established practice of averaging periodic changes to identify overall trends, commonly used in fields such as financial analysis and population studies, where month-over-month or year-over-year comparisons reveal growth or decline patterns [57]. This trend-based approach allows us to capture general contagion patterns rather than predicting exact future cases, aligning with the aim of flexible and resilient demand adjustments. While the CI serves as a valuable indicator for anticipated demand changes, it may not account for extreme situations, especially unknown-unknown uncertainties that cannot be predicted from historical data. To address these, robust optimization is integrated into the URSP model, enhancing MSC resilience by preparing for worst-case scenarios beyond the scope of demand adjustment based solely on CI values.

To develop the CI prediction model, data are collected from 973 districts in Türkiye during and post-pandemic periods. The dataset includes seven features believed to influence the CI, selected based on expert opinions from various fields, including medical doctors, industrial engineers, sociologists, psychologists, and lawyers. The response variable is the CI. Explanations of the addressed features are provided in Table 2. Due to page limitations, comprehensive data on the features and CI values are accessible via the following link: [https://github.com/data-re/viableMSC].

$$CI_i = \frac{1}{n-1}\sum_{t=1}^{n-1}\left(\frac{C_{i,t+1} - C_{i,t}}{C_{i,t}}\right) \tag{57a}$$

where

- CI_i is the contagion index for region i.
- $C_{i,t}$ is the number of infected individuals in region i during week t.
- n is the total number of weeks
- $\frac{C_{i,t+1}-C_{i,t}}{C_{i,t}}$ represents the rate of increase/decrease in the number of infected individuals from week t to week $t+1$.

Using this formula, the CI for each region is calculated by taking the average of the weekly increase/decrease rates over the given period ($n = 5$).

As shown in Table 2, most of the features are strongly associated with the socio-political decisions made by governments over the long term.

Fig. 3. The schematic representation of the medical kit allocation problem.

Table 2
Features with their definitions and explanations.

Feature	Definition	Explanation
Population Density per km² (F1)	The number of people living per square kilometer in a given area.	Population density is a crucial factor in the contagion level of diseases. Higher population density can lead to increased contact rates among individuals, facilitating the transmission of the virus.
Youth Population Density per km² (F2)	The number of individuals aged under 18 living per square kilometer.	The density of the youth population is significant because younger individuals often have higher social interaction rates, both within and outside educational institutions, potentially accelerating the contagion level of diseases.
Proportion of Highly Educated Citizens (F3)	The percentage of the population with a bachelor's degree or higher education.	The level of education may influence adherence to public health guidelines and the ability to access and comprehend health information. Educated populations might exhibit different behavior patterns that can affect the contagion level of diseases.
Rule Violation/ Citation Frequency (F4)	The frequency of rule violations or citations issued in an area.	The number of rule violations can indicate the level of compliance with public health measures. Higher rates of non-compliance can lead to more rapid and widespread transmission of the diseases.
Doctor Density per 1000 People (F5)	The number of doctors available per 1000 inhabitants.	Access to medical care is essential during a pandemic. A higher density of doctors can lead to better management of cases, early detection of infections, and more efficient healthcare responses, potentially mitigating the contagion level of diseases.
Total Number of Hospitals (F6)	The total number of hospitals in a district.	The availability of hospitals is a critical factor in a pandemic response. More hospitals can mean better healthcare infrastructure, capacity to treat more patients, and quicker isolation of infected individuals.
Number of Enclosed Social Venues (F7)	The number of enclosed social venues such as theaters, cinemas, and shopping malls.	Enclosed social venues are potential hotspots for contagion level of diseases due to high foot traffic and close contact among individuals. The presence of these venues can significantly influence the contagion dynamics in a region.

Therefore, examining the impact of these policies is crucial for gaining managerial insights into the MSC viability in preparation for future pandemics in the post-COVID era.

While Case 1 represents the normal situation where there is no pandemic or contagion, Cases 2, 3, 4, and 5 are created based on different policy combinations. To assess the impact of governmental policies on MSC viability, Taguchi's orthogonal array is used. This method incorporates three factors, each at two levels, using an L4 orthogonal array to systematically examine the effects of multiple factors at different levels with a minimal number of experiments. Each factor corresponds to a different policy, with the policy combinations represented in the L4 design as distinct cases. Specifically, the L4 design is utilized to efficiently evaluate both the interactions and the main effects of the policies.

As depicted in Table 3, each row of the design corresponds to a distinct combination of policies implemented by the government over the long term. For example, Case 2 involves the combination of the three policies: (i) implementing deterrent penalties, (ii) encouraging higher education policies, and (iii) strategies to attract and retain healthcare professionals.

Factor 1: Changes in Legislation
Level 1: Implementation of deterrent penalties
Level 2: Amendments of laws in line with public demands
Factor 2: Higher Education Policies
Level 1: Implementation of policies encouraging higher education
Level 2: Restriction of higher education resources
Factor 3: Healthcare Policies
Level 1: Implementation of policies to attract and retain healthcare professionals
Level 2: Budget cuts in the healthcare sector

The Taguchi method, renowned for its efficiency in optimizing design parameters with a limited number of experiments rather than exhaustive testing [12], is employed in this study. This approach utilizes orthogonal arrays for experimental design and the Signal-to-Noise (S/N) ratio to measure the quality of outcomes, emphasizing robustness in performance [72]. The orthogonal array allows for the simultaneous assessment of multiple parameters. Eq. (58) is used to compute the S/N ratio, evaluating the influence of factors and their levels on the overall cost.

$$(S/N)_{ij} = -10log_{10}\left(\frac{\sum z_{ij}^2}{n}\right) \ \forall i,j \tag{58}$$

4.3. Parameter settings

To assess the demand scenarios, three different distributions are considered as illustrated in Fig. 4: normal distribution (ND) for normal situations; left skew distribution (Sk-1) for rare and unprecedented situations; and highly left skew distribution (Sk-2) for extreme situations. Additionally, three levels of scenario counts are examined: 20, 40, and 100, represented as S=20, S =40, and S =100, respectively. These scenarios are generated by considering each distribution separately, ensuring a comprehensive analysis of demand variations.

Five distinct cases are investigated under the three different distribution types for each scenario. Case 1 represents the baseline scenario where demand follows a normal distribution without any contagion potential. Cases 2, 3, 4, and 5 are developed based on specific policy implementations aimed at managing the contagion level of disease. For each case, six different approaches, as depicted in Fig. 2, are evaluated through the proposed methodology.

Further, the results are analyzed for five different levels of the upper bound for the shortages (ϵ), while varying the confidence levels (α) for the CVaR method.

To prevent stockouts in the medical kit allocation problem, relatively small ϵ values of 0.25, 0.30, 0.35, and 0.50 are selected. Additionally, a

Table 3
Factors with their levels and corresponding Taguchi orthogonal array design.

Factors and Levels				L4 design		
Factors	Levels			Factor 1	Factor 2	Factor 3
	1	**2**	Case 2	1	1	1
Factor 1	[600, 1100]	[900, 1600]	Case 3	1	2	2
Factor 2	[20, 24]	[14, 18]	Case 4	2	1	2
Factor 3	[3, 5]	[2, 3]	Case 5	2	2	1

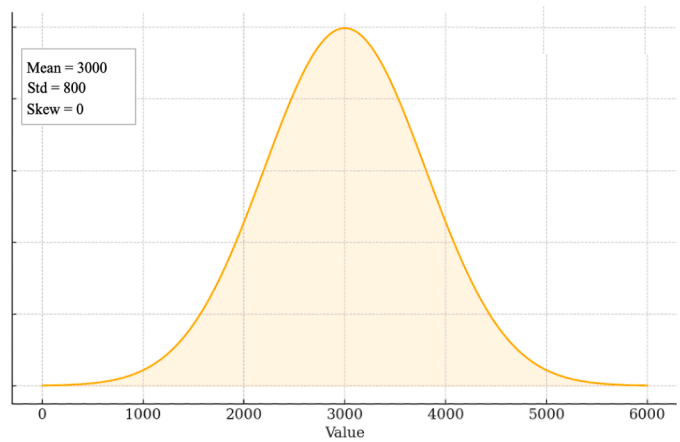

(a) Normal distribution (ND) for normal situations

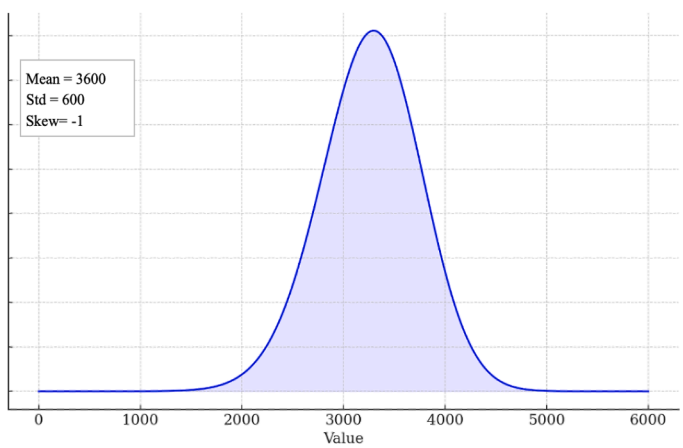

(b) Skewed-1 distribution (Sk-1) for rare and unprecedented situations

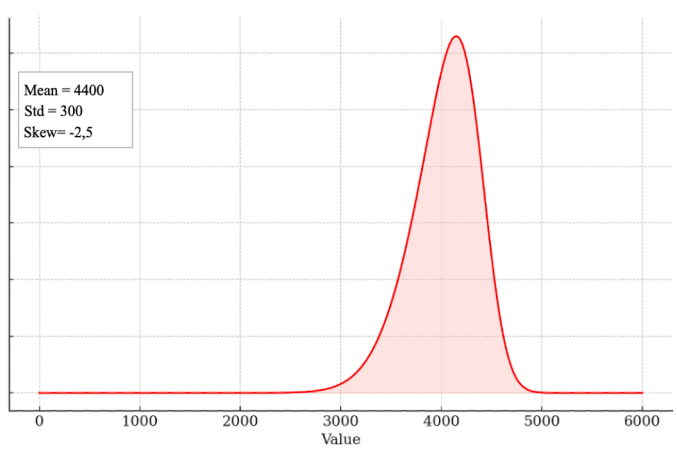

(c) Skewed-2 distribution (Sk-2) for extreme situations

Fig. 4. The comparison of the distributions.

higher value of 0.95 is included in the analysis to observe the variability in the results. Alongside this, α levels representing the confidence levels for CVaR are examined from 0.0 to 0.1, allowing a thorough assessment of risk aversion impacts. The parameter network for the proposed methodology for a number of scenarios setting (i.e. $|S| = 20$) is illustrated in Fig. 5.

4.4. Computational results

4.4.1. Results for CI prediction

The primary goal of the Taguchi design is to analyze the impact of various policies on the MSC viability. Following the implementation of these policies, there are changes in the values of features. Therefore, there is a need to predict the CI values based on the altered feature values resulting from the implemented policies.

To predict the CI values, a correlation-based feature selection (CFS) method is initially used to identify features that significantly impact the CI. The CFS algorithm evaluates the relevance of each feature in the dataset by calculating the correlation between each feature and the class feature, as well as the inter-correlation among features [40]. It selects a subset of features that are highly correlated with the class feature but not with each other [37]. A threshold correlation value of 0.05 is set, and three features -F4, F3, and F5-are selected for predicting the CI.

Three distinct ML algorithms, mentioned in Section 3.1, are employed for regression prediction: (i) RF, (ii) GB, and (iii) KNN. The most effective algorithm among these is selected to predict the CI values resulting from the implementation of the policies described in the previous section.

For each algorithm, specific hyperparameter settings are defined, as detailed in Table 4. The configuration that yields the best results is highlighted in bold and selected for use as the input parameter. Additionally, once the input parameters are established, the performance of the algorithms is assessed using three metrics: (i) Coefficient of Determination (R^2), (ii) Root Mean Square Error (RMSE), and (iii) Mean Absolute Error (MAE). A higher R^2 value indicates better model performance, whereas lower values of RMSE and MAE suggest superior accuracy of an algorithm.

The metrics are computed using the following equations.

$$R^2 = 1 - \frac{\sum_{i=1}^{n}(y_i - \hat{y}_i)^2}{\sum_{i=1}^{n}(y_i - \overline{y_i})^2} \tag{59}$$

$$RMSE = \sqrt{\sum_{i=1}^{n}(y_i - \hat{y}_i)^2 \Big/ n} \tag{60}$$

$$MAE = \sum_{i=1}^{n}|y_i - \hat{y}_i| \Big/ n \tag{61}$$

Phyton code comparing the ML algorithms is accessible via the following link: [https://github.com/data-re/viableMSC].

The hyperparameter setting and results are presented in Tables 4 and 5 respectively.

For the RF algorithm, three input parameters are considered: (i) Number of trees in the forest (NT), (ii) Maximum depth of the trees (MDT), and (iii) Minimum number of samples required to split an internal node (MNS). For the GB algorithm, three input parameters are also considered: (i) Number of boosting stages to perform (NBS), (ii) Learning rate (LR), and (iii) Maximum depth of the individual regression estimators (MD). For the KNN algorithm, two input parameters are considered: (i) Number of neighbors (NN) and (ii) Weight function (WF) used in prediction.

After the input parameters have been determined, the algorithms are applied to the dataset, which is split into 80 % for training and 20 % for testing. The metric values achieved by the algorithms are presented in Table 5.

The experimental design is applied solely to the city of Trabzon/Türkiye. Potential outcomes for each case are determined by examining similar research studies following the implementation of these policies. When similar studies are examined in this context, it is observed that implementing deterrent penalties for rule violations can reduce infractions by 10–30 %, as demonstrated by research on the deterrent effects of harsher punishments [49]. Enhancing educational policies and

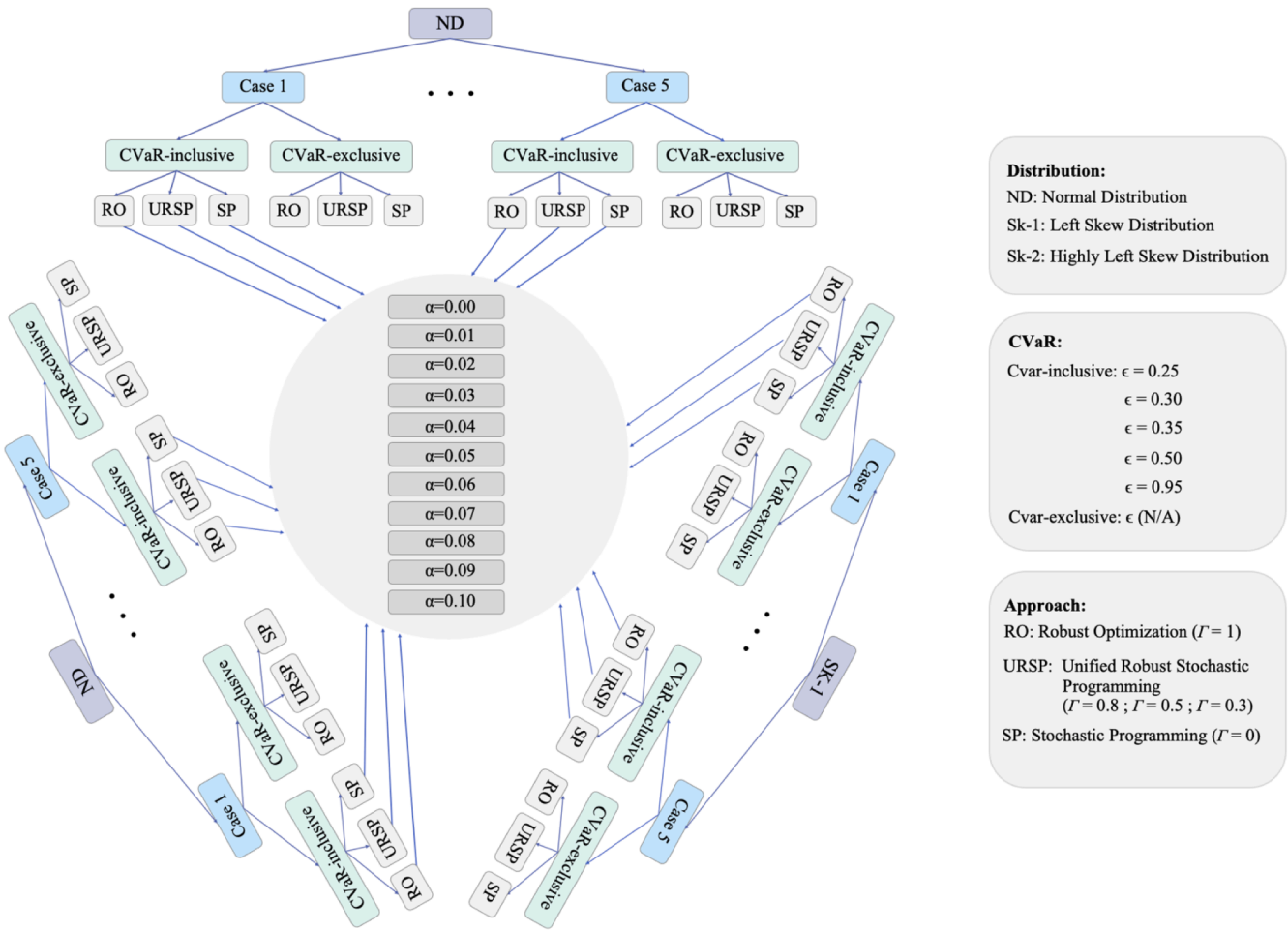

Fig. 5. The parameter network for $|S| = 20$.

Table 4
Hyperparameter settings for algorithms.

Algorithms	Hyperparameters		
RF	NT	MDT	MNS
	[100; 200; 300; **400**]	[None; **10**; 20; 30]	[2; 5; **10**]
GB	NBS	LR	MD
	[**100**; 200; 300]	[0.01; **0.05**; 0.1]	[**3**; 5;10]
KNN	NN	WF	
	[3; 5; **7**; 10]	['uniform'. '**distance**']	

*Best values denoted in bold.

Table 5
The metrics results for algorithms.

	R^2	RMSE	MAE
RF	0.88	9.66	7.45
GB	**0.89**	**9.5**	**7.25**
KNN	0.86	10.77	8.31

*Best values denoted in bold.

investments can increase the proportion of highly educated citizens by 10–20 % leading to a more informed public that is better equipped to adhere to health guidelines and thereby potentially reducing the contagion level of diseases. Additionally, improving doctor density by 20–30 % through expanded medical training programs and recruitment initiatives enhances healthcare accessibility and response capabilities during epidemics and pandemics [7]. This increase in the healthcare workforce ensures better management of the pandemic and reduces the overall infection rate. Based on these studies and the policies considered, cases are created by determining how each feature would change if these policies were implemented. The CI values, indicating the contagion level of the disease in a specific planning period (e.g., weekly or bi-weekly), obtained for cases 2, 3, 4, and 5, are presented in Table 6.

4.4.2. Results for modeling approaches

In this section, the computational experiments are conducted for modeling approaches to analyze the impact of the CI on the MSC viability across multiple cases and varying parameter values. In this regard, the proposed model is coded by using GAMS® 23.6/CPLEX solver on a computer with 2.4 GHz Intel(R) Core™ i7–3630QM CPU and 16 GB of RAM. The addressed medical kit allocation problem is solved through different parameter settings for the computational analysis, resulting in 12,600 runs. These runs consist of three different scenario levels, three different distributions, five cases, six different ϵ categories, 11 different α levels, and five different Γ values, corresponding to three modeling approaches: RO, SP, and URSP. All computations are performed using the CPLEX solver. All optimal results are achieved in seconds. The experimental results are provided on GitHub [https://github.com/data-re/viableMSC]. The computational results achieved by the RO, URSP, and SP approaches with CVaR for the addressed three distributions are shown in Table 7 for $|S| = 100$ with $\epsilon = 0.25$. The results obtained by the same modeling approaches without risk aversion are given in Table 8 for $|S| = 100$.

From Tables 7 and 8, it is evident that in terms of objective function values, the RO approach produces the most conservative solutions,

Table 6
I values obtained for cases.

Case 2								
Districts of Trabzon	Population Density per km²	Youth Population Density per km²	Proportion of Highly Educated Citizens	Rule Violation/ Citation Frequency	Doctor Density per 1000 People	Total Number of Hospitals	Number of Enclosed Social Venues	CI %
District 1	336	101	23	988	4	2	4	**73.57**
District 2	105	31	21	1022	3	1	4	**85.08**
District 3	25	8	20	712	3	1	2	**62.14**
District 4	26	8	20	656	4	1	0	**52.16**
District 5	27	8	20	848	5	2	3	**70.34**
District 6	167	50	21	1003	4	1	4	**80.86**
District 7	1398	419	23	932	5	10	14	**72.81**
District 8	162	48	22	868	3	1	4	**70.54**
District 9	80	24	20	743	4	1	0	**64.66**
District 10	195	59	21	719	3	1	2	**62.14**
District 11	208	62	21	910	4	1	6	**70.07**
Case 3								
Districts of Trabzon	Population Density per km²	Youth Population Density per km²	Proportion of Highly Educated Citizens	Rule Violation/ Citation Frequency	Doctor Density per 1000 People	Total Number of Hospitals	Number of Enclosed Social Venues	CI %
District 1	336	101	17	988	2	2	4	**75.53**
District 2	105	31	16	1022	2	1	4	**87.04**
District 3	25	8	15	712	3	1	2	**63.02**
District 4	26	8	14	656	2	1	0	**51.91**
District 5	27	8	15	848	3	2	3	**71.72**
District 6	167	50	15	1003	2	1	4	**82.81**
District 7	1398	419	18	932	3	10	14	**74.13**
District 8	162	48	15	868	2	1	4	**72.5**
District 9	80	24	14	743	2	1	0	**64.6**
District 10	195	59	15	719	2	1	2	**63.02**
District 11	208	62	17	910	2	1	6	**72.03**
Case 4								
Districts of Trabzon	Population Density per km²	Youth Population Density per km²	Proportion of Highly Educated Citizens	Rule Violation/ Citation Frequency	Doctor Density per 1000 People	Total Number of Hospitals	Number of Enclosed Social Venues	CI %
District 1	336	101	23	1352	2	2	4	**100.14**
District 2	105	31	21	1540	2	1	4	**110.52**
District 3	25	8	20	1147	3	1	2	**91.51**
District 4	26	8	20	1018	2	1	0	**85.66**
District 5	27	8	20	1036	3	2	3	**83.59**
District 6	167	50	21	1285	2	1	4	**95.89**
District 7	1398	419	23	1362	3	10	14	**111.09**
District 8	162	48	22	1130	2	1	4	**86.62**
District 9	80	24	20	954	2	1	0	**73.99**
District 10	195	59	21	1062	2	1	2	**83.49**
District 11	208	62	21	1282	2	1	6	**95.89**
Case 5								
Districts of Trabzon	Population Density per km²	Youth Population Density per km²	Proportion of Highly Educated Citizens	Rule Violation/ Citation Frequency	Doctor Density per 1000 People	Total Number of Hospitals	Number of Enclosed Social Venues	CI %
District 1	336	101	17	1352	4	2	4	**103.61**
District 2	105	31	16	1540	3	1	4	**114.31**
District 3	25	8	15	1147	3	1	2	**94.4**
District 4	26	8	14	1018	4	1	0	**86.1**
District 5	27	8	15	1036	5	2	3	**84.96**
District 6	167	50	15	1285	4	1	4	**99.35**
District 7	1398	419	18	1362	5	10	14	**113.92**
District 8	162	48	15	1130	3	1	4	**90.08**
District 9	80	24	14	954	4	1	0	**74.42**
District 10	195	59	15	1062	3	1	2	**85.44**
District 11	208	62	17	1282	4	1	6	**99.35**

followed by the URSP and SP approaches. The objective function values of the RO approach remain unaffected by changes in the distribution. However, an increase in the objective function values is observed for the URSP and SP approaches as the skewness of the distribution increases.

When examining Table 7 in detail, it becomes clear that as the α level increases, the objective function values of the SP and URSP approaches show a slight increase. In contrast, the objective function values of the RO approach remain unchanged regardless of variations in α levels and distributions. Additionally, the total amount of unsatisfied demand generally tends to increase for each risk aversion approach with CVaR as the skewness of the distribution rises. Among all these modeling approaches, the SP approach consistently yields the lowest amount of unsatisfied demand. Furthermore, Table 8 shows that while the RO approach is overly conservative, the SP approach consistently provides the lowest total amount of unsatisfied demand. Therefore, the URSP approach offers a better tradeoff between cost efficiency and minimizing

Table 7
Results of RO, URSP, and SP approaches with ($\epsilon = 0.25$) for S = 100 with respect to selected α values and cases.

Distribution	Cases	Γ value	Modeling Approach	α Value	Obj	Total expected amount of unsatisfied demand for SP part	Total expected amount of surplus inventory for SP part	Total expected amount of kits produced for SP part	The amount of unsatisfied demand for RO part	The amount of surplus inventory for RO part	Total amount of kits produced for RO part	The amount of medical kits allocated at the first-stage	CPU
ND	Case 1	Γ=1	RO	0.05	3,925,500	–	–	–	28,500	0	0	103,500	0.19
		Γ=1	RO	0.10	3,925,500	–	–	–	28,500	0	0	103,500	0.2
		Γ=0.8	URSP	0.05	3,831,999.03	1094.1	32,978.63	0	31,500	0	3380	97,120	0.26
		Γ=0.8	URSP	0.10	3,832,023.16	1035.55	33,058.08	0	31,500	0	3242	97,258	0.25
		Γ=0.5	URSP	0.05	3,390,210.12	6504.85	8564.85	1439.48	33,000	0	33,144	65,856	0.28
		Γ=0.5	URSP	0.10	3,391,640.53	6555.63	8503.38	1500.23	33,000	0	33,317	65,683	0.28
		Γ=0.3	URSP	0.05	2,901,336.73	10,181.6	3563.87	3286.75	33,000	0	43,669	55,331	0.3
		Γ=0.3	URSP	0.10	2,903,081.22	10,181.92	3546.45	3278	33,000	0	43,678	55,322	0.31
		Γ=0	SP	0.05	2,107,924.75	12,579.53	1799.23	5433.17	–	–	–	49,022	0.55
		Γ=0	SP	0.10	2,111,148.85	12,449.03	1829.9	5480.35	–	–	–	49,136	0.51
	Case 3	Γ=1	RO	0.05	7,087,139	–	–	–	56,885	0	20,678	150,000	0.25
		Γ=1	RO	0.10	7,087,139	–	–	–	56,885	0	20,678	150,000	0.27
		Γ=0.8	URSP	0.05	6,625,243.59	4167.21	42,232.61	547.35	56,880	0	20,683	150,000	0.38
		Γ=0.8	URSP	0.10	6,626,060.37	4117.82	42,203.94	568.08	56,885	0	20,678	150,000	0.39
		Γ=0.5	URSP	0.05	5,794,338.46	11,114.08	14,895.95	2417.83	56,885	0	56,832	113,846	0.25
		Γ=0.5	URSP	0.10	5,796,673.46	11,162.95	14,825.09	2516.1	56,885	0	57,050	113,628	0.29
		Γ=0.3	URSP	0.05	4,958,893.81	17,592.37	6120.41	5653	56,885	0	75,321	95,357	0.31
		Γ=0.3	URSP	0.10	4,961,712.72	17,452.94	6173.96	5554.98	56,885	0	75,030	95,648	0.29
		Γ=0	SP	0.05	3,601,960.01	21,644.99	3124.83	9288.8	–	–	–	84,673	0.52
		Γ=0	SP	0.10	3,607,218.61	21,417.93	3170.65	9390.67	–	–	–	84,844	0.52
	Case 5	Γ=1	RO	0.05	8,689,008.3	–	–	–	66,886	0	50,701	150,000	0.15
		Γ=1	RO	0.10	8,689,008.3	–	–	–	66,886	0	50,701	150,000	0.15
		Γ=0.8	URSP	0.05	7,916,061.29	8998.4	28,296.9	1615.8	66,886	0	50,701	150,000	0.38
		Γ=0.8	URSP	0.10	7,917,266.31	8933	28,262.1	1646.4	66,886	0	50,701	150,000	0.54
		Γ=0.5	URSP	0.05	6,733,590.46	12,873.87	17,769.82	2731.25	66,886	0	66,219	134,482	0.33
		Γ=0.5	URSP	0.10	6,736,162.82	12,910.64	17,654.19	2861.85	66,886	0	66,502	134,199	0.3
		Γ=0.3	URSP	0.05	5,763,063.42	20,613.53	7260.11	6472.87	66,886	0	88,210	112,491	0.31
		Γ=0.3	URSP	0.10	5,766,142.7	20,416.33	7349.86	6366.83	66,886	0	87,817	112,884	0.29
		Γ=0	SP	0.05	4,184,521.67	25,377.7	3726.72	10,764.32	–	–	–	99,902	0.63
		Γ=0	SP	0.10	4,190,480.61	25,080.35	3803.12	10,827.07	–	–	–	100,213	0.49
Distribution	Cases	Γ value	Modeling Approach	α Value	Obj	Total expected amount of unsatisfied demand for SP part	Total expected amount of surplus inventory for SP part	Total expected amount of kits produced for SP part	The amount of unsatisfied demand for RO part	The amount of surplus inventory for RO part	Total amount of kits produced for RO part	The amount of medical kits allocated at the first-stage	CPU
Sk-1	Case 1	Γ=1	RO	0.05	3,925,500	–	–	–	28,500	0	0	103,500	0.15
		Γ=1	RO	0.10	3,925,500	–	–	–	28,500	0	0	103,500	0.15
		Γ=0.8	URSP	0.05	3,826,296.5	652.45	27,117.57	0	31,500	0	2648	97,852	0.26
		Γ=0.8	URSP	0.10	3,826,296.5	652.45	27,117.57	0	31,500	0	2648	97,852	0.25
		Γ=0.5	URSP	0.05	3,397,648.87	6478.38	4778.53	536.02	33,000	0	29,849	69,151	0.23
		Γ=0.5	URSP	0.10	3,398,298.91	6494.08	4731.9	555.7	33,000	0	29,931	69,069	0.27
		Γ=0.3	URSP	0.05	2,942,448.87	10,291.15	1334.07	1280.8	33,000	0	37,851	61,149	0.4
		Γ=0.3	URSP	0.10	2,943,439.25	10,285.97	1327.32	1335.23	33,000	0	37,907	61,093	0.29
		Γ=0	SP	0.05	2,215,811.36	13,129.15	492.15	2417.88	–	–	–	56,332	0.51
		Γ=0	SP	0.10	2,217,422.9	13,230.28	471.32	2493.93	–	–	–	56,134	0.52
	Case 3	Γ=1	RO	0.05	7,087,139.4	–	–	–	56,885	0	20,678	150,000	0.14
		Γ=1	RO	0.10	7,087,139.4	–	–	–	56,885	0	20,678	150,000	0.26
		Γ=0.8	URSP	0.05	6,621,468.79	4498.02	31,708.15	228.53	56,885	0	20,678	150,000	0.37
		Γ=0.8	URSP	0.10	6,621,861.62	4439.52	31,669.25	248.13	56,885	0	20,678	150,000	0.39
		Γ=0.5	URSP	0.05	5,805,104.43	11,022.58	8329.44	888.25	56,885	0	51,241	119,437	0.26
		Γ=0.5	URSP	0.10	5,806,207.49	11,005.62	8255.15	914.92	56,885	0	51,325	119,353	0.28

(*continued on next page*)

Table 7 (*continued*)

Distribution	Cases	Γ value	Modeling Approach	α Value	Obj	Total expected amount of unsatisfied demand for SP part	Total expected amount of surplus inventory for SP part	Total expected amount of kits produced for SP part	The amount of unsatisfied demand for RO part	The amount of surplus inventory for RO part	Total amount of kits produced for RO part	The amount of medical kits allocated at the first-stage	CPU
		Γ=0.3	URSP	0.05	5,026,374.05	17,609.78	2325.91	2163.52	56,885	0	65,107	105,571	0.28
		Γ=0.3	URSP	0.10	5,027,994.51	17,582.59	2321.89	2216.7	56,885	0	65,137	105,541	0.26
		Γ=0	SP	0.05	3,782,585.33	22,523.99	857.08	4140.48	–	–	–	97,211	0.52
		Γ=0	SP	0.10	3,785,130.58	22,729.67	818.08	4274.8	–	–	–	96,832	0.49
	Case 5	Γ=1	RO	0.05	8,689,008.3	–	–	–	66,886	0	50,701	150,000	0.27
		Γ=1	RO	0.10	8,689,008.3	–	–	–	66,886	0	50,701	150,000	0.26
		Γ=0.8	URSP	0.05	7,915,750.18	9393.8	15,311.13	615.78	66,886	0	50,701	150,000	0.39
		Γ=0.8	URSP	0.10	7,916,269.42	9366.82	15,315.33	646.95	66,886	0	50,701	150,000	0.38
		Γ=0.5	URSP	0.05	6,744,119.75	12,705.32	9905.81	1011.93	66,886	0	59,814	140,887	0.3
		Γ=0.5	URSP	0.10	6,745,280.96	12,648.76	9847.69	1015.37	66,886	0	59,819	140,882	0.25
		Γ=0.3	URSP	0.05	5,838,761.65	20,554.92	2770.2	2464.72	66,886	0	76,252	124,449	0.39
		Γ=0.3	URSP	0.10	5,840,635.22	20,538.53	2758.47	2533.37	66,886	0	76,316	124,385	0.24
		Γ=0	SP	0.05	4,390,928.54	26,506.62	1009.21	4796.03	–	–	–	114,405	0.5
		Γ=0	SP	0.10	4,393,742.58	26,650.32	975.55	4923.67	–	–	–	114,100	0.52
Distribution	Cases	Γ value	Modeling Approach	α Value	Obj	Total expected amount of unsatisfied demand for SP part	Total expected amount of surplus inventory for SP part	Total expected amount of kits produced for SP part	The amount of unsatisfied demand for RO part	The amount of surplus inventory for RO part	Total amount of kits produced for RO part	The amount of medical kits allocated at the first-stage	CPU
Sk-2	Case 1	Γ=1	RO	0.05	2,580,000	–	–	–	114,000	0	0	18,000	0.15
		Γ=1	RO	0.10	2,580,000	–	–	–	114,000	0	0	18,000	0.13
		Γ=0.8	URSP	0.05	2,433,261.85	79,856.28	1878.75	0	118,014	0	0	13,986	0.14
		Γ=0.8	URSP	0.10	2,433,261.85	79,856.28	1878.75	0	118,014	0	0	13,986	0.12
		Γ=0.5	URSP	0.05	2,199,454.56	80,136.75	123.23	0	120,050	0	0	11,950	0.15
		Γ=0.5	URSP	0.10	2,199,454.56	80,136.75	123.23	0	120,050	0	0	11,950	0.15
		Γ=0.3	URSP	0.05	2,039,827.66	80,235	88.48	0	120,183	0	0	11,817	0.13
		Γ=0.3	URSP	0.10	2,039,827.66	80,235	88.48	0	120,183	0	0	11,817	0.13
		Γ=0	SP	0.05	1,800,099.13	80,528.15	48.63	0	–	–	–	11,484	0.14
		Γ=0	SP	0.10	1,800,099.13	80,528.15	48.63	0	–	–	–	11,484	0.13
	Case 3	Γ=1	RO	0.05	4,447,054	–	–	–	195,571	1	0	31,993	0.14
		Γ=1	RO	0.10	4,447,054	–	–	–	195,571	1	0	31,993	0.13
		Γ=0.8	URSP	0.05	4,194,392.1	137,027.03	3239.2	0	202,806	2	0	24,758	0.27
		Γ=0.8	URSP	0.10	4,194,392.1	137,027.03	3239.2	0	202,806	1	0	24,758	0.14
		Γ=0.5	URSP	0.05	3,791,334.2	137,538.14	214.31	0	206,341	0	0	21,222	0.13
		Γ=0.5	URSP	0.10	3,791,334.2	137,538.14	214.31	0	206,341	0	0	21,222	0.14
		Γ=0.3	URSP	0.05	3,516,163.07	137,712.75	153.92	0	206,576	0	0	20,987	0.14
		Γ=0.3	URSP	0.10	3,516,163.07	137,712.75	153.92	0	206,576	0	0	20,987	0.14
		Γ=0	SP	0.05	3,102,905.43	138,232.42	84.59	0	–	–	–	20,398	0.14
		Γ=0	SP	0.10	3,102,905.43	138,232.42	84.59	0	–	–	–	20,398	0.13
	Case 5	Γ=1	RO	0.05	5,230,395	–	–	–	229,932	2	0	37,656	0.15
		Γ=1	RO	0.10	5,230,395	–	–	–	229,932	2	0	37,656	0.15
		Γ=0.8	URSP	0.05	4,933,121.16	161,127.96	3754.91	0	238,526	0	0	29,061	0.19
		Γ=0.8	URSP	0.10	4,933,121.16	161,127.96	3754.91	0	238,526	0	0	29,061	0.16
		Γ=0.5	URSP	0.05	4,459,020.68	161,722.67	249.61	0	242,626	0	0	24,961	0.15
		Γ=0.5	URSP	0.10	4,459,020.68	161,722.67	249.61	0	242,626	0	0	24,961	0.17
		Γ=0.3	URSP	0.05	4,135,455.43	161,929.21	179.16	0	242,903	0	0	24,684	0.12
		Γ=0.3	URSP	0.10	4,135,455.43	161,929.21	179.16	0	242,903	0	0	24,684	0.14
		Γ=0	SP	0.05	3,649,521.74	162,550.88	97.82	0	–	–	–	23,981	0.25
		Γ=0	SP	0.10	3,649,521.74	162,550.88	97.82	0	–	–	–	23,981	0.14

Table 8
Results for selected cases of RO, URSP, and SP approaches without risk aversion for S = 100.

Distribution	Cases	Γ value	Modeling Approach	Obj	Total expected amount of unsatisfied demand for SP part	Total expected amount of surplus inventory for SP part	Total expected amount of kits produced for SP part	The amount of unsatisfied demand for RO part	The amount of surplus inventory for RO part	Total amount of kits produced for RO part	The amount of medical kits allocated at the first-stage	CPU
ND	Case 1	Γ=1	RO	2,580,000	–	–	–	114,000	0	0	18,000	0.13
		Γ=0.8	URSP	2,335,765.65	57,316.22	3185.75	0	120,895	0	0	11,105	0.14
		Γ=0.5	URSP	1,948,432.81	58,520.4	517.92	0	124,767	0	0	7233	0.13
		Γ=0.3	URSP	1,683,566.96	58,801.35	372.88	0	125,193	0	0	6807	0.14
		Γ=0	SP	1,284,858	59,736.57	164.1	0	–	–	–	5663	0.25
	Case 3	Γ=1	RO	4,447,054	–	–	–	195,572	1	0	31,993	0.13
		Γ=0.8	URSP	4,026,674.16	98,453.86	5500.91	0	208,035	1	0	19,529	0.16
		Γ=0.5	URSP	3,359,038.14	100,623.72	894.77	0	214,811	0	0	12,753	0.25
		Γ=0.3	URSP	2,902,496.41	101,114.25	644.3	0	215,552	0	0	12,012	0.14
		Γ=0	SP	2,215,247.9	102,756.55	283.59	0	–	–	–	10,009	0.14
	Case 5	Γ=1	RO	5,230,395	–	–	–	229,933	1	0	37,656	0.13
		Γ=0.8	URSP	4,735,970.76	115,809.73	6384.43	0	244,695	0	0	22,892	0.14
		Γ=0.5	URSP	3,950,886.24	118,359.68	1041.38	0	252,588	0	0	14,999	0.14
		Γ=0.3	URSP	3,414,210.23	118,944.56	750.27	0	253,464	0	0	14,123	0.14
		Γ=0	SP	2,606,357.12	120,904.22	328.93	0	–	–	–	11,742	0.25
Sk-1	Case 1	Γ=1	RO	2,580,000	–	–	–	114,000	0	0	18,000	0.13
		Γ=0.8	URSP	2,357,763.75	62,495.73	2776.85	0	120,332	0	0	11,668	0.16
		Γ=0.5	URSP	2,004,550.56	62,940.9	327.02	0	123,227	0	0	8773	0.13
		Γ=0.3	URSP	1,763,336.44	63,143.6	203.73	0	123,553	0	0	8447	0.14
		Γ=0	SP	1,400,591.63	63,419	86.13	0	–	–	–	8054	0.13
	Case 3	Γ=1	RO	4,447,054	–	–	–	195,571	1	0	31,993	0.14
		Γ=0.8	URSP	4,064,221.07	107,260.13	4783.74	0	207,022	0	0	20,542	0.24
		Γ=0.5	URSP	3,454,976.37	108,057.99	564.6	0	212,038	0	0	15,525	0.22
		Γ=0.3	URSP	3,038,930.39	108,417.23	351.83	0	212,610	0	0	14,953	0.14
		Γ=0	SP	2,413,269.36	108,895.49	149.1	0	–	–	–	14,272	0.14
	Case 5	Γ=1	RO	5,230,395	–	–	–	229,932	1	0	37,656	0.13
		Γ=0.8	URSP	4,780,103.24	126,148.46	5547.02	0	243,490	0	0	24,097	0.14
		Γ=0.5	URSP	4,063,672.88	127,087.84	655.4	0	249,321	0	0	18,266	0.14
		Γ=0.3	URSP	3,574,594.36	127,508.37	407.93	0	249,989	0	0	17,598	0.13
		Γ=0	SP	2,839,129.09	128,073.05	172.61	0	–	–	–	16,798	0.13
Distribution	Cases	Γ value	Modeling Approach	Obj	Total expected amount of unsatisfied demand for SP part	Total expected amount of surplus inventory for SP part	Total expected amount of kits produced for SP part	The amount of unsatisfied demand for RO part	The amount of surplus inventory for RO part	Total amount of kits produced for RO part	The amount of medical kits allocated at the first-stage	CPU
Sk-2	Case 1	Γ=1	RO	2,580,000	–	–	–	114,000	0	0	18,000	0.13
		Γ=0.8	URSP	2,433,261.85	79,856.28	1878.75	0	118,014	0	0	13,986	0.12
		Γ=0.5	URSP	2,199,454.56	80,136.75	123.23	0	120,050	0	0	11,950	0.15
		Γ=0.3	URSP	2,039,827.66	80,235	88.48	0	120,183	0	0	11,817	0.13
		Γ=0	SP	1,800,099.13	80,528.15	48.63	0	–	–	–	11,484	0.13
	Case 3	Γ=1	RO	4,447,054	–	–	–	195,571	1	0	31,993	0.13
		Γ=0.8	URSP	4,194,392.1	137,027.03	3239.2	0	202,806	0	0	24,758	0.14
		Γ=0.5	URSP	3,791,334.2	137,538.14	214.31	0	206,341	0	0	21,222	0.14
		Γ=0.3	URSP	3,516,163.07	137,712.75	153.92	0	206,576	0	0	20,987	0.14
		Γ=0	SP	3,102,905.43	138,232.42	84.59	0	–	–	–	20,398	0.13
	Case 5	Γ=1	RO	5,230,395	–	–	–	229,932	1	0	37,656	0.15
		Γ=0.8	URSP	4,933,121.16	161,127.96	3754.91	0	238,526	0	0	29,061	0.16
		Γ=0.5	URSP	4,459,020.68	161,722.67	249.61	0	242,626	0	0	24,961	0.17
		Γ=0.3	URSP	4,135,455.43	161,929.21	179.16	0	242,903	0	0	24,684	0.14
		Γ=0	SP	3,649,521.74	162,550.88	97.82	0	–	–	–	23,981	0.14

unsatisfied demand.

When examining all experimental results, as expected, a slight decrease in the objective function value is observed, as the scenario count increases for all modeling approaches [https://github.com/data-re/viableMSC]. This trend aligns with expectations and is clearly shown in Fig. 6. The figure compares the objective function values obtained through URSP approaches at different levels of Γ for ϵ=0.25. It presents results across scenario sizes of |S|=20, |S|=40, and |S|=100, considering all addressed distributions and cases.

When examining the objective function values in Fig. 6, it becomes clear that as the distribution becomes more skewed, the differences resulting from the number of scenarios diminish significantly. Although similar trends are observed across different Γ levels, the objective function tends to be lower at smaller Γ values. Overall, slightly better objective function values are consistently obtained for |S|=100 in all addressed cases and distributions, further justifying the focus on this scenario size in the subsequent analyses.

Upon reviewing all the experimental results, in risk aversion approaches, it is observed that the objective function values increase up to $\alpha = 0.1$ and then converge to a certain value. This pattern is illustrated in Fig. 7, showing the change in objective function values for the URSP approach with Γ=0.5 across various distributions. The computational results are visualized for different α values, with $|S| = 100$ and $\epsilon = 0.25$, for all cases. From Fig. 7, similar trend in α levels are observed despite

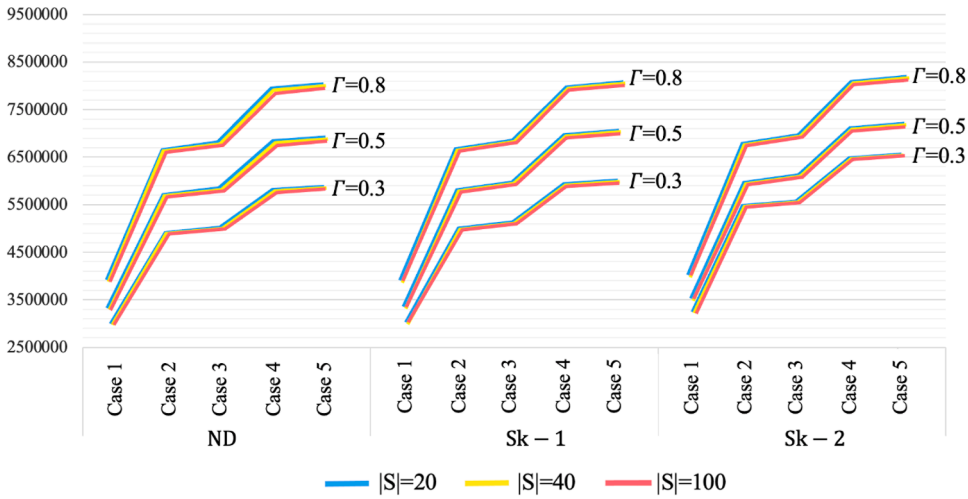

Fig. 6. The comparison of objective function values obtained by URSP approaches for $\epsilon = 0.25$.

differences in objective function values. These patterns change as the distribution structure becomes more skewed for each case. Consequently, in the most skewed distribution, the objective function value converges more rapidly with smaller α values.

The changes in objective function values across all modeling approaches and three distributions, with varying ϵ values, are illustrated in Fig. 8 for Cases 1, 3, and 5, with $|S| = 100$. From this figure, it is observed that in the RO approach, all three distributions yield the same objective function values for all ϵ values. In contrast, in the SP and URSP approaches, the objective function value increases with the skewness of the distribution. The objective values show a similar trend across different ϵ values for all modeling approaches, regardless of the implemented cases. However, a considerable increase is observed in the URSP, and especially in the RO approaches. Therefore, it can be stated that when the robust approach is taken into consideration in modeling, conservative solutions are achieved. This impact becomes more pronounced when only the RO part is considered, resulting in over conservative solutions.

Fig. 9 examines the relationship between unsatisfied demand, which is an important indicator for assessing MSC viability, and objective function values across modeling approaches which are constructed according to varying Γ values for all cases. In this regard, Fig. 9(a and b) depicts the results for risk aversion approaches with $\epsilon = 0.25$, and $\epsilon = 0.50$, respectively while Fig. 9(c) illustrates the results for approaches without CVaR. As seen in Fig. 9, the approaches incorporating CVaR lead to fewer inventory stockouts with higher objective function values. However, it is also evident that as the ϵ values increase, so do the shortage levels. In addition to this, it is deduced that the objective values provided by each approach slightly decrease as the ϵ value increases, and the lowest objective values are achieved in the case without CVaR. In similar way, the lowest objective function value for each case is obtained in the SP (corresponds to Γ=0). approaches, while the highest objective function value is achieved in the RO approaches (corresponds to Γ=1). It is not surprising that the RO approach results in overly conservative solutions compared to other approaches.

As a reminder, prior research has examined both robust optimization and two-stage stochastic programming to support day-ahead and secondary decisions in medical kit allocation. Yet, each method faces specific challenges: stochastic optimization can be computationally demanding due to extensive scenario sizes, while robust optimization may lead to overly conservative outcomes [79]. As evidenced by the computational analyses conducted, this study introduces an innovative URSP model that merges the advantages of these approaches, aiming to achieve low expected costs alongside robust system performance. With adjustable weights for the stochastic and robust components in the objective function, the model offers flexibility, allowing decision-makers or SC managers to adapt based on their preferences. Given that the viability of MSC settings must account for unknown-unknown uncertainties, this approach strengthens MSC viability by allowing decision-makers to set robustness levels (Γ) from 0 to 1.

Fig. 9 demonstrates that, in risk aversion approaches, lower amounts of unsatisfied demand are achieved, as expected, and these approaches are well-suited for ensuring the viability of the MSC. However, from the sustainability aspect of MSC, modeling approaches that provide low costs should not be overlooked to ensure MSC viability. Fig. 9 illustrates that the SP approaches successfully achieve the lowest unsatisfied demand at the lowest cost. However, SC managers relying solely on SP approaches address only known-unknown uncertainty. A critical consideration in this context is the incorporation of unknown-unknown uncertainty, which is vital for the viability of the MSC. Consequently, while a robustness level (Γ) of 1 may lead to overly conservative cost outcomes, adopting a smaller Γ value (e.g., 0.8) proves more advantageous for SC managers. The proposed URSP approach enables them to consider both types of uncertainty, leading to a more balanced modeling strategy.

Overall, the implementation of the URSP approach with CVaR is recommended, as it provides solutions with reasonable cost levels while still maintaining low backorder levels. In a nutshell, while CVaR is a promising risk aversion method, the combination of CVaR and RO approach within the context of risk aversion can be preferred to mitigate the risk caused by disruptions for the sake of MSC viability.

Figs. 10–12 illustrate the differences in the objective function values between the weighted average solutions of the SP and RO approaches and the URSP solutions for cases 1, 3, and 5, respectively. Specifically, Fig. 10 presents the results for case 1, Fig. 11 for case 3, and Fig. 12 for case 5. These figures compare the approaches with and without CVaR, considering different levels of skewness in the distribution.

From these figures, the preferred risk aversion approach (using CVaR for this purpose, also referred to as risk measurement) clearly highlights the distinction between the proposed URSP approach and a linear combination of SP and RO approaches, making the difference between them reasonable. This difference is achieved with the proposed URSP approach, and as the difference increases, the level of unsatisfied demand decreases. The goal is for this difference to be as large as possible.

As observed from these figures, in the approaches without CVaR, the objective function values between the weighted average solutions of the SP and RO approaches and the URSP solutions are very close for the addressed cases. As the ε value increases, the effect of CVaR diminishes, indicating how dependent our proposed method is on risk aversion.

Similarly, as the skewness of the distribution increases, the

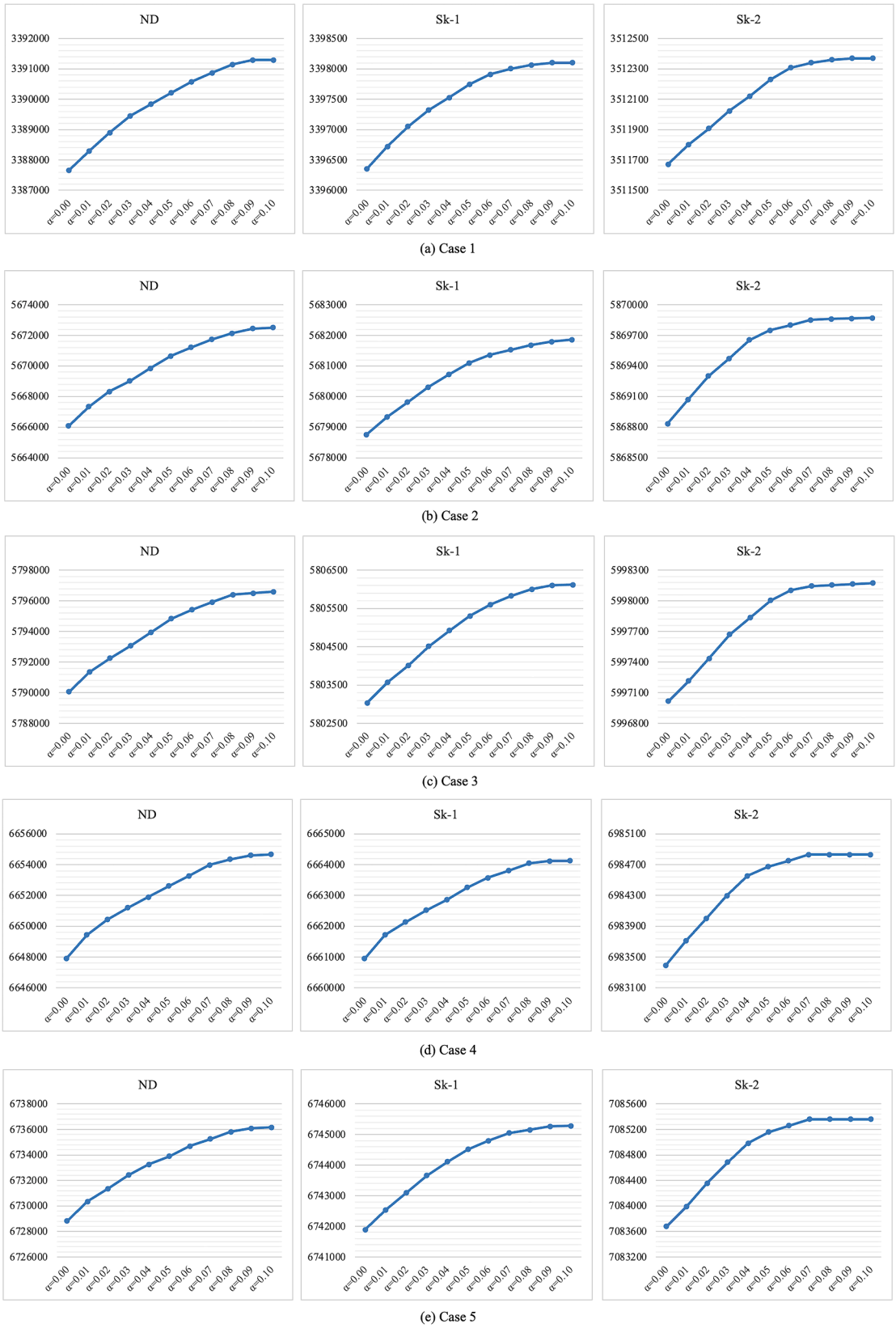

Fig. 7. Objective function values achieved by URSP (Γ=0.5) approach for different α values across various distributions for $|S| = 100$, $\epsilon = 0.25$.

difference between the weighted average solutions of the SP and RO approaches and the URSP solutions narrows because, as skewness increases, demand tends to concentrate near the extreme values. Consequently, the solution obtained from the stochastic approach is expected to be closer to the robust solution. In a stochastic setting, demand is typically centered around the average; however, as skewness increases, demand becomes more concentrated around the peak (in a narrower range). Therefore, the stochastic solution converges toward the robust

Fig. 8. The changes in objective function values across all modeling approaches and three distributions, with varying ϵ values for different cases.

solutions as skewness increases.

In the approaches with CVaR, as the value of ε decreases, the gap between the URSP solutions and the weighted average solutions of the SP and RO approaches widens. Additionally, when comparing the computational results presented in Figs. 10–12, it is shown that as demand increases, the gap between the URSP solutions and the weighted average solutions of the SP and RO approaches narrows.

Overall, as the ϵ value decreases, the unsatisfied demand level also decreases, leading to a growing difference between the URSP solutions and the linear combination solutions of the SP and RO approaches. This relationship underscores that a greater difference correlates with a lower shortage level, as measured by the shortage level indicator. Furthermore, it can be stated that the URSP approach is particularly effective where CVaR has a significant influence. This highlights the fact that MSC involves urgent needs, meaning risk aversion approaches must be considered in this type of supply chain. MSC requires such considerations, which is why it can be concluded that the URSP model operates properly with the CVaR approach. As a result, an effective model for MSC has been developed, incorporating CVaR to ensure high effectiveness even in extreme situations by facilitating the reduction of unsatisfied demand. This underscores the significance of the proposed URSP approach for MSC.

Fig. 13 illustrates the allocation of medical kits at the first stage under varying CVaR and Γ values, demonstrating how different risk aversion and robustness levels affect first-stage decision-making in the model. As anticipated, an increase in Γ leads to more conservative production decisions, with higher initial allocations of medical kits. This outcome aligns with the expectation that as Γ grows, the model becomes more robust to unknown-unknown uncertainties, thus prioritizing resilience over cost efficiency. Consequently, higher Γ values reflect an increase in first-stage production as the model aims to mitigate potential shortages that could arise from unexpected disruptions.

Additionally, variations in ϵ reveal how CVaR influences the model's aversion to stockouts. Lower ϵ values correlate with stricter constraints on unsatisfied demand, prompting higher initial production levels to preemptively address potential shortages. Conversely, in the situation where CVaR is not applied (ϵ (N/A)), the model tends to produce significantly lower first-stage allocations, as the lack of risk aversion allows for a cost-driven, less conservative approach.

An interesting observation from the figure is that as demand intensifies (reflecting extreme situations), the differences in solutions across various Γ values reduce. This convergence suggests that under extreme demand fluctuations, all model approaches—irrespective of robustness level—yield relatively similar first-stage production decisions. This outcome indicates that when facing highly unpredictable demand, the impact of Γ-based conservatism reduces, as all approaches lean towards securing sufficient initial production to maintain supply chain viability.

In summary, the figure underscores that increasing Γ reinforces conservative production decisions to hedge against unknown-unknown risks, and lowering ϵ values similarly promotes stockout aversion through increased first-stage production. However, under extreme demand scenarios, the approaches yield converging solutions, reflecting a unified focus on resilience across the models. This analysis highlights the balance between cost and robustness, where both CVaR and robustness parameters contribute significantly to strategic first-stage production planning.

As stated earlier, Case 1 corresponds to the situation in which contagion is not considered. Thus, it is expected to have the lowest objective function values. Other cases represent the combination of the

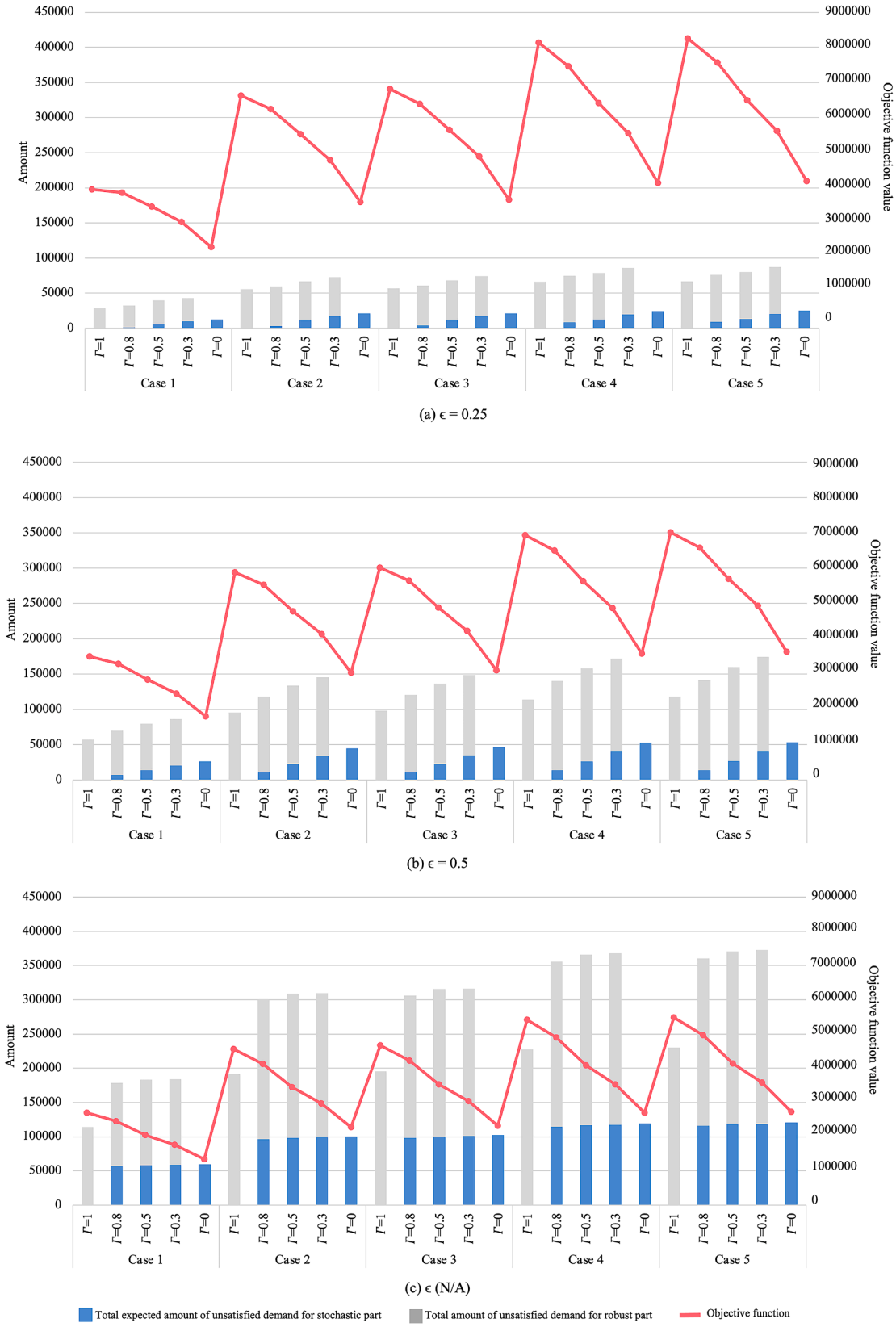

Fig. 9. The relationship between unsatisfied demand and surplus inventory amount with objective function values across all cases and approaches (for $\epsilon = 0.25$, $\epsilon = 0.5$ and $\epsilon = \text{N/A}$).

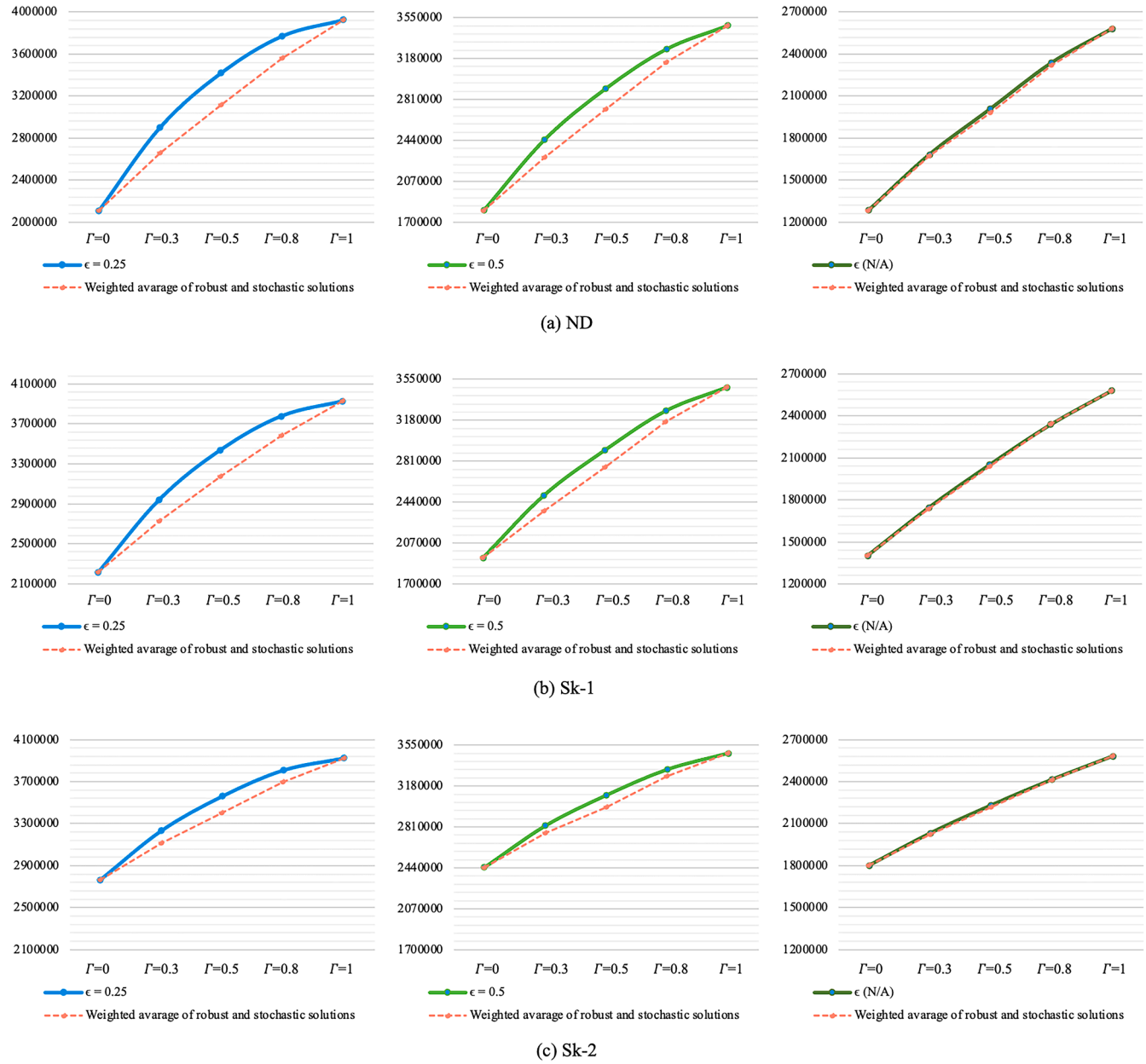

Fig. 10. The differences in the objective function values between the weighted average solutions of the SP and RO approaches and URSP approaches for Case 1.

policies mentioned in Section 4.2. Accordingly, for these cases, CI values are determined based on the specified policy combinations. It is known that these CI values directly affect the demand. Consequently, these modeling approaches exhibit higher objective function values as the number of cases increases but maintain similar tendencies. Nevertheless, the highest objective function values are obtained for Case 5.

Upon comparing the results obtained from these cases, it is observed that the objective function values for Case 2 and Case 3 are quite similar. Likewise, Case 4 and Case 5 also exhibit close values. However, there is a noticeable difference between the values of Case 2 and 3 compared to Case 4 and 5. To determine the policies (factors) causing this difference, a more comprehensive analysis is conducted for a selected situation where $\Gamma = 0.5$; $\epsilon = 0.25$. The computational results are provided in Table 9 and Fig. 14 with respect to controllable factors and their levels. This analysis demonstrates which controllable factors have the most influence on the overall cost and which levels critically affect the results.

The first factor "Changes in Legislation" has the most significant influence on the results. From this perspective, this governmental policy should be prioritized when developing future policies. The second factor, "Higher Education Policies" shows a smaller impact, suggesting that while it has some effect, it is less critical. Lastly, the third factor, "Healthcare Policies" demonstrates minimal influence on the results. This result indicates that it is not essential for future governmental legislation in this context.

5. Discussion and managerial insights

This section provides an in-depth analysis of the study's findings and their implications for achieving MSC viability. Each research question (RQ-1 to RQ-4) is directly answered, followed by reasoning and managerial guidance.

The URSP framework introduced in this study integrates these two philosophies. By adjusting a robustness parameter (Γ), decision-makers can shift between SP and RO. In environments where both unknown-unknown and known-unknown uncertainties may arise, URSP provides the flexibility needed to maintain MSC viability.

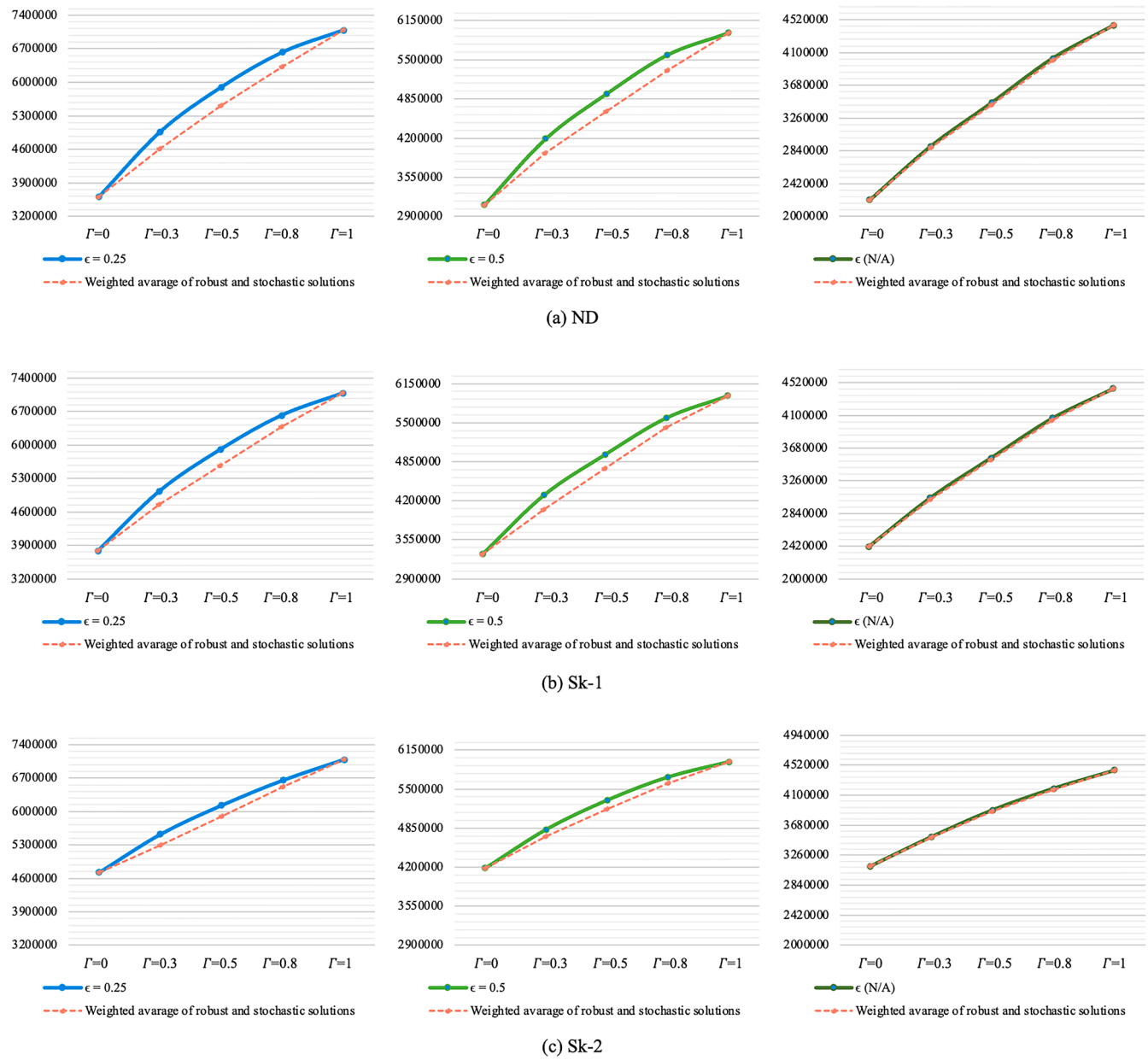

Fig. 11. The differences in the objective function values between the weighted average solutions of the SP and RO approaches and URSP approaches for Case 3.

Answer to RQ-1: The URSP approach, especially when combined with CVaR, is the most effective. Purely stochastic methods handle known-unknown uncertainties well but may fail under unforeseen disruptions. Purely robust methods prepare the system for the worst case but can be overly conservative and costly. By blending these methods, URSP allows decision-makers to dynamically adjust the balance between cost-efficiency and resilience. Lower Γ values rely more on SP (useful when historical data exist), while higher Γ values invoke more robust features (essential when black swan events or unknown-unknown uncertainties emerge).

Managerial recommendations:

- **Adaptive robustness policies:** It may be useful to establish guidelines that allow adjustments to Γ as data reliability or environmental signals change. During stable conditions, relying more on stochastic solutions could be beneficial. As uncertainty grows, considering increases to Γ may ensure adequate robustness.
- **Combined analytics and workshops:** It could be helpful to conduct scenario analysis sessions to observe how different Γ values affect outcomes. Such sessions may assist decision-makers in reaching consensus on appropriate robustness levels.

Answer to RQ-2: Risk aversion approaches, particularly those involving CVaR, improve resilience by reducing the frequency and severity of shortages. CVaR looks beyond a simple probability threshold (as VaR does) and considers how severe shortages can become if they occur. This aspect is vital for MSCs, where occasional extreme shortages can have severe consequences. However, increasing risk aversion may raise costs. Parameters such as the upper bound on shortages (ϵ) and the CVaR confidence level (α) can be tuned to maintain a balance. This ensures the MSC is robust enough to handle tail-end risks without incurring unnecessarily high expenses during normal conditions.

Managerial recommendations:

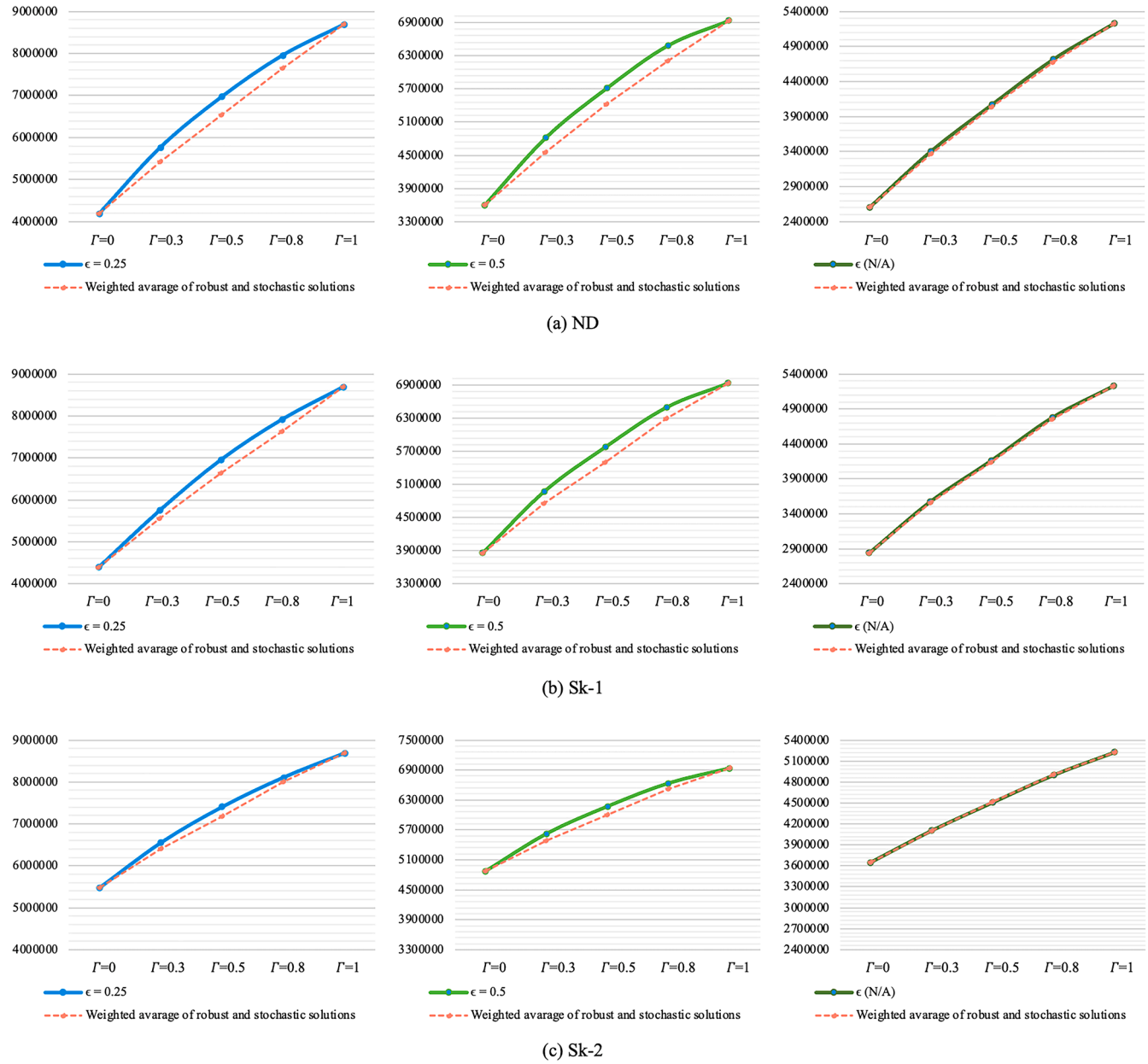

Fig. 12. The differences in the objective function values between the weighted average solutions of the SP and RO approaches and URSP approaches for Case 5.

- **Integrate CVaR constraints**: It may be advantageous to include CVaR in planning efforts to account for both the likelihood and magnitude of severe shortages.
- **Calibration of ϵ and α:** Considering moderate parameter levels at the outset may help in achieving an acceptable balance between cost and service reliability. Gradual refinements may be appropriate as experience with demand patterns grows.
- **Responsive adjustment:** Slightly easing risk aversion in stable periods might help contain costs, while increasing risk constraints when signs of volatility arise may safeguard essential supplies.

Answer to RQ-3: A combination of deterrent penalties for non-compliance, higher education initiatives, and strategies for attracting and retaining healthcare professionals is most effective. Deterrent penalties reduce contagion rates, stabilizing demand. Better-educated healthcare workers improve data quality, patient management, and operational responsiveness. This alignment of policies results in more predictable demand, shifting uncertainty from unknown-unknown to known-unknown territory, where scenario-based methods are more effective.

Managerial recommendations:

- **Advocacy for supportive policies:** Although direct policy enforcement is not within managerial control, sharing insights on how certain measures (e.g., deterrent penalties) enhance MSC stability may encourage policymakers to support beneficial changes.
- **Collaborations with stakeholders:** It may be worthwhile to partner with public health authorities and educational institutions. Such collaboration could help ensure that policy adjustments lead to a well-prepared workforce and improved compliance, thereby reducing uncertainty for the MSC.

Answer to RQ-4: As uncertainty intensifies or demand distributions become skewed, purely stochastic models may produce higher costs or fail to provide stable solutions. In contrast, robust and URSP models maintain more reliable performance under these conditions. By

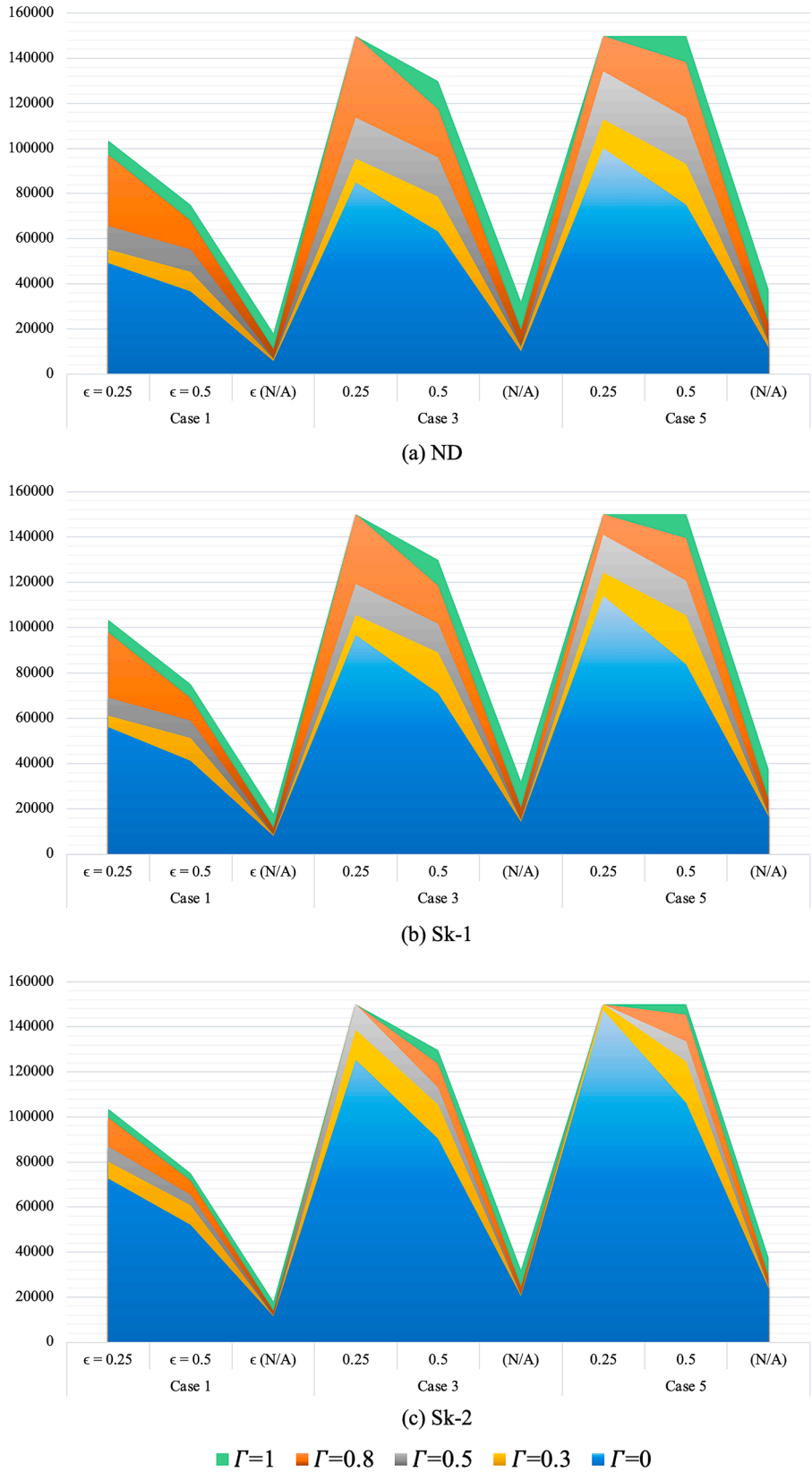

Fig. 13. First-stage medical kit allocation decisions for cases 1, 3, and 5 with respect to different ϵ and $\mathbf{\Gamma}$ values.

adjusting Γ and employing CVaR, URSP can handle a wide range of uncertainty structures. Managers could thus achieve stable costs and service levels, even as the environment shifts from relying on known data (known-unknown) to facing completely unfamiliar events (unknown-unknown).

Managerial recommendations:

Table 9
Taguchi design results with respect to S/N.

Cases	L_4	Factor 1	Factor 2	Factor 3	ND		Sk-1		Sk-2	
					Obj.	S/N	Obj.	S/N	Obj.	S/N
Case 2	1	1	1	1	5,672,548.5	−135.076	5,681,859.5	−135,090	5,869,949.0	−135.373
Case 3	2	1	1	2	5,796,673.5	−135.264	5,806,207.5	−135,278	5,998,175.6	−135.560
Case 4	3	2	1	2	6,655,159.9	−136.463	6,664,328.4	−136,475	6,984,966.8	−136.883
Case 5	4	2	2	1	6,736,162.8	−136.568	6,745,281.0	−136,580	7,085,359.5	−137.007

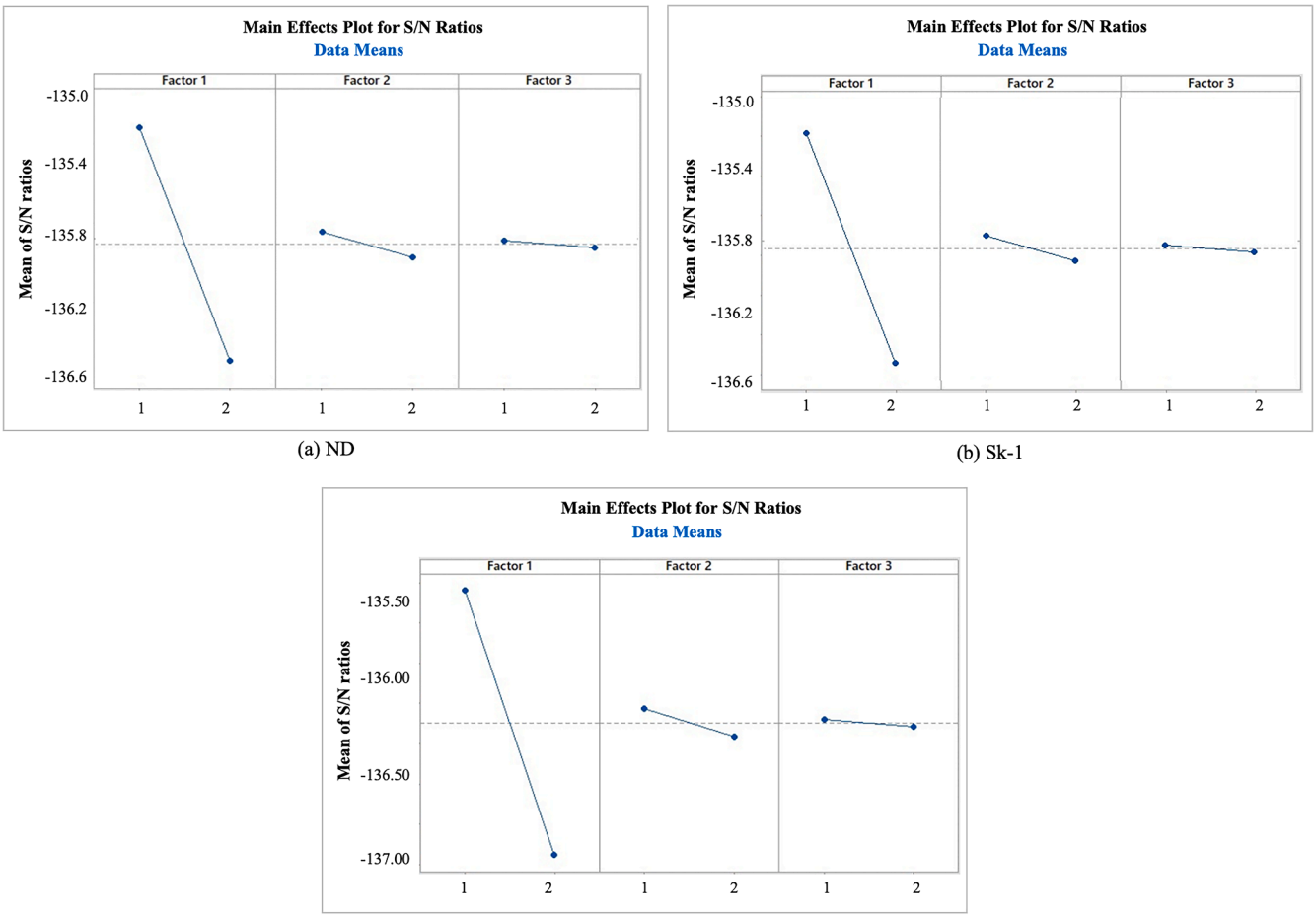

(a) ND (b) Sk-1 (c) Sk-2

Fig. 14. Main effects plot for S/N ratios with respect to distributions.

- **Continuous monitoring of demand:** It may be prudent to track changes in demand patterns on a regular basis. If anomalies appear, considering increases in robustness or risk aversion might help in maintaining reliable service.
- **Use of advanced analytics:** Employing machine learning tools could assist in identifying when historical data no longer represents the future accurately. This information may guide timely adjustments to model parameters, supporting ongoing MSC viability.

These findings suggest that relying on a single approach may not be sufficient under all conditions. URSP models, with their capacity to consider both known-unknown uncertainties through SP and unknown-unknown uncertainties through RO, could offer a more flexible framework. Incorporating CVaR into these models may help in managing severe shortage risks by allowing adjustments to maintain acceptable costs. Moreover, encouraging supportive governmental policies and strengthening internal capabilities (e.g., workforce training, inventory management) may contribute to a more predictable demand environment, thereby reducing uncertainty. The proposed integrated approach appears to provide a comprehensive strategy for achieving MSC viability. In a context where pandemics and unforeseen disruptions remain possible, employing such a combined and adaptive methodology might be valuable.

6. Concluding remarks

This study proposes a methodology that integrates ML algorithms with an URSP approach to ensure the viability of MSCs by addressing the medical kit allocation problem during an epidemic or pandemic. The effectiveness of various modeling approaches is examined within the context of MSC viability by considering different types of uncertainty, including known-unknown and unknown-unknown uncertainties. To control unsatisfied demand levels, the CVaR method and RO approach are employed for risk aversion.

To illustrate the practical application and effectiveness of the proposed methodology, a comprehensive case study is conducted in

Türkiye. Data from 973 districts are utilized to compare three different ML algorithms, with GB identified as the most effective. Using the GB algorithm, CI calculations are performed for 11 districts in Trabzon/Türkiye, considering various potential policy combinations to develop different cases. As the first step of the methodology, the CI values are predicted through the selected ML algorithm. Following that, the six modeling approaches are executed for the considered cases under varying risk level settings for multiple distribution types. The computational results reveal that incorporating the CVaR approach is essential, as it minimizes unsatisfied demand to achieve MSC viability. The adaptability of the proposed URSP model, which combines the strengths of SP and RO with adjustable robustness levels, provides SC managers with a flexible tool to balance cost efficiency and viability. By enabling adjustments for both known and unknown uncertainties, the URSP model allows SC managers to prioritize their needs, offering a resilient approach that is particularly valuable in volatile and uncertain environments. Overall, the URSP model combined with CVaR is suggested to achieve MSC viability by considering both resilience and sustainability aspects in the post-COVID era. Furthermore, the proposed URSP model, which integrates CVaR, demonstrates strong performance even in extreme conditions while enabling the reduction of unsatisfied demand. This highlights the critical importance of the proposed model in enhancing MSC viability.

This study contributes to existing academic literature in the following aspects:

i. **Theoretical contribution:** This study addresses the medical kit allocation problem within the context of MSC viability. It integrates ML algorithms with a novel URSP model by emphasizing sustainability and resilience from an operational perspective rather than a structural (re)design perspective.
ii. **Managerial contribution:** By conducting extensive experiments with multiple modeling approaches under both known-unknown and unknown-unknown uncertainties, this study provides valuable insights for ensuring MSC viability and mitigating risks during epidemics or pandemics. Additionally, sensitivity analysis is performed to assess the impact of different risk aversion levels and disruption severity on MSC viability.
iii. **Methodological contribution:** A comprehensive methodology is developed, beginning with an ML algorithm for predicting contagion levels, followed by modeling approaches incorporating risk aversion and uncertainty types. Risk aversion is addressed through RO, the CVaR method, or both, identifying the most effective strategies for controlling maximum allowable shortage levels and maintaining a veneer of normalcy.

Despite its contributions, this study acknowledges several limitations that suggest directions for future research:

- **Objective function**: The MSC viability is only considered from the overall cost perspective. Future studies could expand the scope to include other conflicting objectives, such as minimizing carbon emissions, reducing overall cost, and addressing workload imbalance.
- **Diversity of ML algorithms and adjustment index**: While this study primarily utilizes GB, employing other ML algorithms might enhance CI predictions for different countries, such as the United States and countries in the European Union. Furthermore, different demand adjustment index considering contagion level of diseases can be developed and employed instead of CI.
- **Large-size problem instance**: The considered MSC network includes two stages with one supplier and one warehouse. Future studies could adapt heuristics/metaheuristics approaches to solve larger-sized problems with more complex network structure.

CRediT authorship contribution statement

Ömer Faruk Yılmaz: Writing – review & editing, Writing – original draft, Validation, Supervision, Methodology, Investigation, Formal analysis, Conceptualization. **Yongpei Guan:** Validation, Supervision, Project administration, Methodology, Investigation. **Beren Gürsoy Yılmaz:** Writing – original draft, Visualization, Validation, Methodology, Investigation, Data curation. **Fatma Betül Yeni:** Writing – original draft, Visualization, Resources, Investigation, Formal analysis, Data curation. **Gökhan Özçelik:** Writing – original draft, Resources, Methodology, Formal analysis.

Declaration of competing interest

The authors declare that they have no known competing financial interests or personal relationships that could have appeared to influence the work reported in this paper.

Acknowledgement

This work was supported by the Scientific and Technological Research Council of Türkiye (TUBITAK) BIDEB 2219.

Data availability

No data was used for the research described in the article.

References

[1] Ahmadi H, Samany NN, Ghanbari A, Argany M. Designing a bi-level emergency medical centers' chain to increase the resilience of EMS's supply-chain using ACO-QAP: a case study of Tabriz. Int J Disaster Risk Reduct 2022;82:103259.
[2] Aldrighetti R, Battini D, Ivanov D. Efficient resilience portfolio design in the supply chain with consideration of preparedness and recovery investments. Omega 2023;117:102841.
[3] Alizadeh M, Abad ARKK, Jahani H, Makui A. Prevention of post-pandemic crises: a green sustainable and reliable healthcare supply chain network design for emergency medical products. J Clean Prod 2024;434:139702.
[4] Alizadeh M, Pishvaee MS, Jahani H, Paydar MM, Makui A. Viable healthcare supply chain network design for a pandemic. Ann Oper Res 2023;328(1):35–73.
[5] Bentéjac C, Csörgő A, Martínez-Muñoz G. A comparative analysis of gradient boosting algorithms. Artif Intell Rev 2021;54:1937–67.
[6] Broekaert JB, Hafiz F, Jayaraman R, La Torre D. Managing resilience and viability of supranational supply chains under epidemic control scenarios. Omega 2024:103234.
[7] Boniol M, Kunjumen T, Nair TS, Siyam A, Campbell J, Diallo K. The global health workforce stock and distribution in 2020 and 2030: a threat to equity and universal health coverage? BMJ Glob Health 2022;7(6):e009316.
[8] Camur MC, Ravi SK, Saleh S. Enhancing supply chain resilience: a machine learning approach for predicting product availability dates under disruption. Expert Syst Appl 2024;247:123226.
[9] Dolgui A, Gusikhin O, Ivanov D, Li X, Stecke K. A network-of-networks adaptation for cross-industry manufacturing repurposing. IISE Trans 2024;56(6):666–82.
[10] Echefaj K, Cherrafi A, Charkaoui A, Gruchmann T, Ivanov D. Firm survivability during long-term disruptions: an adaptation-based view. Supply Chain Manag Int J 2024.
[11] Echefaj K, Charkaoui A, Cherrafi A, Ivanov D. Design of resilient and viable sourcing strategies in intertwined circular supply networks. Ann Oper Res 2024:1–40.
[12] Eskandarpour M, Dejax P, Miemczyk J, Péton O. Sustainable supply chain network design: an optimization-oriented review. Omega 2015;54:11–32.
[13] Esteve M, Aparicio J, Rodriguez-Sala JJ, Zhu J. Random Forests and the measurement of super-efficiency in the context of Free Disposal Hull. Eur J Oper Res 2023;304(2):729–44.
[14] Fahimnia B, Jabbarzadeh A, Ghavamifar A, Bell M. Supply chain design for efficient and effective blood supply in disasters. Int J Prod Econ 2017;183:700–9.
[15] Fereydooni A, Barak S, Sajadi SMA. A novel online portfolio selection approach based on pattern matching and ESG factors. Omega 2024;123:102975.
[16] Gilani H, Sahebi H. A data-driven robust optimization model by cutting hyperplanes on vaccine access uncertainty in COVID-19 vaccine supply chain. Omega 2022;110:102637.
[17] Goodarzian F, Taleizadeh AA, Ghasemi P, Abraham A. An integrated sustainable medical supply chain network during COVID-19. Eng Appl Artif Intell 2021;100:104188.
[18] Han Y, Zhang M, Nan P, Cao J, Huang Q, Ye X, He Z. Two-stage heuristic algorithm for vehicle-drone collaborative delivery and pickup based on medical supplies resource allocation. J King Saud Univ Comput Inf Sci 2023;35(10):101811.

[19] Hasani A, Khosrojerdi A. Robust global supply chain network design under disruption and uncertainty considering resilience strategies: a parallel memetic algorithm for a real-life case study. Transp Res Part E Logist Transp Rev 2016;87:20–52.
[20] Hasani A, Mokhtari H, Fattahi M. A multi-objective optimization approach for green and resilient supply chain network design: a real-life case study. J Clean Prod 2021;278:123199.
[21] Hosseini S, Ivanov D, Dolgui A. Review of quantitative methods for supply chain resilience analysis. Transp Res Part E Logist Transp Rev 2019;125:285–307.
[22] Hussaini Z, Nemati A, Paydar MM. A multi-period multi-season multi-objective mathematical model for guaranteeing the viability of supply chains under fluctuations: a healthcare closed-loop supply chain application. Ann Oper Res 2023:1–46.
[23] Ivanov D. Supply chain viability and the COVID-19 pandemic: a conceptual and formal generalisation of four major adaptation strategies. Int J Prod Res 2021;59(12):3535–52.
[24] Ivanov D. Viable supply chain model: integrating agility, resilience and sustainability perspectives–lessons from and thinking beyond the COVID-19 pandemic. Ann Oper Res 2022;319:1411–31.
[25] Ivanov D. Intelligent digital twin (iDT) for supply chain stress-testing, resilience, and viability. Int J Prod Econ 2023;263:108938.
[26] Ivanov D. Supply chain resilience: conceptual and formal models drawing from immune system analogy. Omega 2024;127:103081.
[27] Ivanov D. Two views of supply chain resilience. Int J Prod Res 2024;62(11):4031–45.
[28] Ivanov D, Dolgui A. Viability of intertwined supply networks: extending the supply chain resilience angles towards survivability. A position paper motivated by COVID-19 outbreak. Int J Prod Res 2020;58(10):2904–15.
[29] Ivanov D, Dolgui A. The shortage economy and its implications for supply chain and operations management. Int J Prod Res 2022;60(24):7141–54.
[30] Ivanov D, Dolgui A, Blackhurst J, Choi TM. Toward supply chain viability theory: from lessons learned through COVID-19 pandemic to viable ecosystems. Int J Prod Res 2023;61(8):2402–15.
[31] Ivanov D, Keskin BB. Post-pandemic adaptation and development of supply chain viability theory. Omega 2023;116:102806.
[32] Kahr M. Determining locations and layouts for parcel lockers to support supply chain viability at the last mile. Omega 2022;113:102721.
[33] Kar S, Mohanty MK, Thakurta PKG. Efficient healthcare supply chain: a prioritized multi-task learning approach with task-specific regularization. Eng Appl Artif Intell 2024;133:108249.
[34] Karadayi-Usta S, Serdarasan S. Supplier selection and capacity allocation in medical tourism service supply chain. OPSEARCH 2023:1–27.
[35] Kargar S, Paydar MM, Safaei AS. A reverse supply chain for medical waste: a case study in Babol healthcare sector. Waste Manag 2020;113:197–209.
[36] Koca E. Two-stage stochastic facility location problem with disruptions and restricted shortages. Comput Ind Eng 2023;183:109484.
[37] Kösesoy İ. Prediction of POMA-G score from spatiotemporal gait parameters. Dicle Üniv Mühendisl Fak Mühendis Derg 2023;14(4):555–61.
[38] Krauss C, Do XA, Huck N. Deep neural networks, gradient-boosted trees, random forests: statistical arbitrage on the S&P 500. Eur J Oper Res 2017;259(2):689–702.
[39] Kumar S, Sharma SC. Integrated model for predicting supply chain risk through machine learning algorithms. Int J Math Eng Manag Sci 2023;8(3).
[40] Kushal TRB, Illindala MS. Correlation-based feature selection for resilience analysis of MVDC shipboard power system. Int J Electr Power Energy Syst 2020;117:105742.
[41] Kück M, Freitag M. Forecasting of customer demands for production planning by local k-nearest neighbor models. Int J Prod Econ 2021;231:107837.
[42] Li G, Yang J, Pu G, Yang L. Multi-objective location-allocation optimization of temporary delivery points for medical supplies during large-scale epidemic outbreaks. Appl Math Model 2024;125:721–37.
[43] Liu M, Ding Y, Chu F, Dolgui A, Zheng F. Robust actions for improving supply chain resilience and viability. Omega 2024;123:102972.
[44] Liu M, Liu Z, Chu F, Dolgui A, Chu C, Zheng F. An optimization approach for multi-echelon supply chain viability with disruption risk minimization. Omega 2022;112:102683.
[45] Lotfi R, Kargar B, Gharehbaghi A, Weber GW. Viable medical waste chain network design by considering risk and robustness. Environ Sci Pollut Res 2022;29:79702–17.
[46] Lotfi R, Mardani N, Ali SS, Pahlevan SM, Davoodi SMR. A robust and risk-averse medical waste chain network design by considering viability requirements. RAIRO-Oper Res 2024;58(2):1473–97.
[47] Ma P, Gong Y, Jin M. Quality efforts in medical supply chains considering patient benefits. Eur J Oper Res 2019;279(3):795–807.
[48] Mercadier M, Lardy JP. Credit spread approximation and improvement using random forest regression. Eur J Oper Res 2019;277(1):351–65.
[49] Moore C, Pierce L. Reactance to transgressors: why authorities deliver harsher penalties when the social context elicits expectations of leniency. Front Psychol 2016;7:550.
[50] Nayeri S, Khoei MA, Rouhani-Tazangi MR, GhanavatiNejad M, Rahmani M, Tirkolaee EB. A data-driven model for sustainable and resilient supplier selection and order allocation problem in a responsive supply chain: a case study of healthcare system. Eng Appl Artif Intell 2023;124:106511.
[51] Özçelik G, Faruk Yılmaz Ö, Betül Yeni F. Robust optimisation for ripple effect on reverse supply chain: an industrial case study. Int J Prod Res 2021;59(1):245–64.
[52] Pazoki M, Samarghandi H, Behroozi M. Increasing supply chain resiliency through equilibrium pricing and stipulating transportation quota regulation. Omega 2024;127:103097.
[53] Petrudi SH, Ahmadi HB, Azareh Y, Liou JJ. Developing a structural model for supply chain viability: a case from a developing country. Oper Manag Res 2024;17(1):324–39.
[54] Pishvaee MS, Razmi J, Torabi SA. An accelerated Benders decomposition algorithm for sustainable supply chain network design under uncertainty: a case study of medical needle and syringe supply chain. Transp Res Part E Logist Transp Rev 2014;67:14–38.
[55] Ramani V, Ghosh D, Sodhi M. Understanding systemic disruption from the Covid-19-induced semiconductor shortage for the auto industry. Omega 2022;113:102720.
[56] Ramezanian R, Behboodi Z. Blood supply chain network design under uncertainties in supply and demand considering social aspects. Transp Res Part E Logist Transp Rev 2017;104:69–82.
[57] Richert, B. (2020). How to calculate average increase. sciencing.com. Retrieved from https://sciencing.com/calculate-average-increase-7479420.html.
[58] Rockafellar RT, Uryasev S. Optimization of conditional value-at-risk. J Risk 2000;2:21–42.
[59] Rockafellar RT, Uryasev S. Conditional value-at-risk for general loss distributions. J Bank Financ 2002;26(7):1443–71.
[60] Rozhkov M, Ivanov D, Blackhurst J, Nair A. Adapting supply chain operations in anticipation of and during the COVID-19 pandemic. Omega 2022;110:102635.
[61] Ruel S, El Baz J, Ivanov D, Das A. Supply chain viability: conceptualization, measurement, and nomological validation. Ann Oper Res 2024:1–30.
[62] Sabouhi F, Pishvaee MS, Jabalameli MS. Resilient supply chain design under operational and disruption risks considering quantity discount: a case study of pharmaceutical supply chain. Comput Ind Eng 2018;126:657–72.
[63] Sardesai S, Klingebiel K. Maintaining viability by rapid supply chain adaptation using a process capability index. Omega 2023;115:102778.
[64] Sawik T. Stochastic optimization of supply chain resilience under ripple effect: a COVID-19 pandemic related study. Omega 2022;109:102596.
[65] Sawik T. A stochastic optimisation approach to maintain supply chain viability under the ripple effect. Int J Prod Res 2023;61(8):2452–69.
[66] Sawik T. Supply chain resilience: multi-tier supply portfolio. Stochastic programming in supply chain risk management: resilience, viability, and cybersecurity. Cham: Springer Nature Switzerland; 2024. p. 69–107.
[67] Sawik T. Supply chain viability: risk-neutral decision-making. Stochastic programming in supply chain risk management: resilience, viability, and cybersecurity. Cham: Springer Nature Switzerland; 2024. p. 155–86.
[68] Sawik T, Sawik B. Risk-averse decision-making to maintain supply chain viability under propagated disruptions. Int J Prod Res 2024;62(8):2853–67.
[69] Simsek S, Dag A, Tiahrt T, Oztekin A. A Bayesian Belief Network-based probabilistic mechanism to determine patient no-show risk categories. Omega 2021;100:102296.
[70] Tüselmann H, Sinkovics RR, Pishchulov G. Towards a consolidation of worldwide journal rankings–a classification using random forests and aggregate rating via data envelopment analysis. Omega 2015;51:11–23.
[71] Wang J, Zhuang Z, Gao D. An enhanced hybrid model based on multiple influencing factors and divide-conquer strategy for carbon price prediction. Omega 2023;120:102922.
[72] Wang S, Huang GH. An integrated approach for water resources decision making under interactive and compound uncertainties. Omega 2014;44:32–40.
[73] Wang X, Jiang R, Qi M. A robust optimization problem for drone-based equitable pandemic vaccine distribution with uncertain supply. Omega 2023;119:102872.
[74] Xie K, Zhu S, Gui P, Chen Y. Coordinating an emergency medical material supply chain with CVaR under the pandemic considering corporate social responsibility. Comput Ind Eng 2023;176:108989.
[75] Xu X, Shen Y, Chen WA, Gong Y, Wang H. Data-driven decision and analytics of collection and delivery point location problems for online retailers. Omega 2021;100:102280.
[76] Yılmaz ÖF, Yeni FB, Yılmaz BG, Özçelik G. An optimization-based methodology equipped with lean tools to strengthen medical supply chain resilience during a pandemic: a case study from Turkey. Transp Res Part E Logist Transp Rev 2023;173:103089.
[77] Zaoui S, Foguem C, Tchuente D, Fosso-Wamba S, Kamsu-Foguem B. The viability of supply chains with interpretable learning systems: the case of COVID-19 vaccine deliveries. Glob J Flex Syst Manag 2023;24(4):633–57.
[78] Zhao C, Guan Y. Data-driven risk-averse stochastic optimization with Wasserstein metric. Oper Res Lett 2018;46(2):262–7.
[79] Zhao C, Guan Y. Unified stochastic and robust unit commitment. IEEE Trans Power Syst 2013;28(3):3353–61.